



THE UNIVERSITY *of* EDINBURGH

Edinburgh Research Explorer

## The genomic basis of host and vector specificity in non-pathogenic trypanosomatids

**Citation for published version:**

Oldrieve, GR, Malacart, B, López-Vidal, J & Matthews, KR 2022, 'The genomic basis of host and vector specificity in non-pathogenic trypanosomatids', *Biology Open*, vol. 11, no. 4.  
<https://doi.org/10.1242/bio.059237>

**Digital Object Identifier (DOI):**

[10.1242/bio.059237](https://doi.org/10.1242/bio.059237)

**Link:**

[Link to publication record in Edinburgh Research Explorer](#)

**Document Version:**

Publisher's PDF, also known as Version of record

**Published In:**

Biology Open

**General rights**

Copyright for the publications made accessible via the Edinburgh Research Explorer is retained by the author(s) and / or other copyright owners and it is a condition of accessing these publications that users recognise and abide by the legal requirements associated with these rights.

**Take down policy**

The University of Edinburgh has made every reasonable effort to ensure that Edinburgh Research Explorer content complies with UK legislation. If you believe that the public display of this file breaches copyright please contact [openaccess@ed.ac.uk](mailto:openaccess@ed.ac.uk) providing details, and we will remove access to the work immediately and investigate your claim.



## RESEARCH ARTICLE

# The genomic basis of host and vector specificity in non-pathogenic trypanosomatids

Guy R. Oldrieve\*, Beatrice Malacart, Javier López-Vidal and Keith R. Matthews

## ABSTRACT

*Trypanosoma theileri*, a non-pathogenic parasite of bovines, has a predicted surface protein architecture that likely aids survival in its mammalian host. Their surface proteins are encoded by genes which account for ~10% of their genome. A non-pathogenic parasite of sheep, *Trypanosoma melophagium*, is transmitted by the sheep ked and is closely related to *T. theileri*. To explore host and vector specificity between these species, we sequenced the *T. melophagium* genome and transcriptome and an annotated draft genome was assembled. *T. melophagium* was compared to 43 kinetoplastid genomes, including *T. theileri*. *T. melophagium* and *T. theileri* have an AT biased genome, the greatest bias of publicly available trypanosomatids. This trend may result from selection acting to decrease the genomic nucleotide cost. The *T. melophagium* genome is 6.3Mb smaller than *T. theileri* and large families of proteins, characteristic of the predicted surface of *T. theileri*, were found to be absent or greatly reduced in *T. melophagium*. Instead, *T. melophagium* has modestly expanded protein families associated with the avoidance of complement-mediated lysis. We propose that the contrasting genomic features of these species is linked to their mode of transmission from their insect vector to their mammalian host.

This article has an associated First Person interview with the first author of the paper.

**KEY WORDS:** *Trypanosoma theileri*, *Trypanosoma melophagium*, Non-pathogenic, Host and vector specificity

## INTRODUCTION

Trypanosomatidae are a family of single-celled eukaryotes of the class Kinetoplastea, which are characterised by a specialised mitochondrial genome, the kinetoplast. Trypanosomatidae are monoxenous (single host) or dixenous (two host) species. Dixenous trypanosomatids are obligate parasites of a broad diversity of animals and plants whilst monoxenous species are largely restricted to insects (Podlipaev, 2001). However, the taxonomy of trypanosomatids cannot be distilled into these two broad categories, as many monoxenous species opportunistically infect vertebrates (Kaufner et al., 2017) and some

dixenous species have subsequently reverted to a monoxenous lifecycle (Schnauffer et al., 2002).

Expansion into vertebrate hosts gave rise to clades of trypanosomatids which represent medical and veterinary threats. Notably, *Trypanosoma cruzi* and *Leishmania* spp. cause important diseases in humans, Chagas disease and Leishmaniasis, respectively. Also, *Trypanosoma brucei* has been subjected to intense molecular and cytological study as two of its subspecies, *T. b. gambiense* and *T. b. rhodesiense*, are causative agents of Human African Trypanosomiasis (HAT) (Cayla et al., 2019). In addition to the medical impact of HAT, other African trypanosome species such as *T. b. brucei*, *Trypanosoma vivax* and *Trypanosoma congolense* cause morbidity and mortality in livestock, constraining agricultural development (Mehlitz and Molyneux, 2019).

The lineage including trypanosomatids diverged from other eukaryotes over a billion years ago (Burki, 2014; Cavalier-Smith, 2010) and possess unique adaptations at the genome level (Maslov et al., 2019). As an example, the *T. brucei* genome comprises 11 megabase chromosomes (Melville et al., 1998) along with ~5 intermediate chromosomes and ~100 mini-chromosomes (Daniels et al., 2010; Wickstead et al., 2004). Nuclear DNA is highly compact, and genes are organised into co-transcribed units, the primary transcripts of which are trans-spliced and polyadenylated to resolve mature mRNA (Clayton, 2019; Parsons et al., 1984). Their distinctive mitochondrial genome, the kinetoplast, consists of mini- (Kleisen and Borst, 1975; Steinert, 1960) and maxicircles (Borst and Fase-Fowler, 1979; Simpson, 1979) that rely upon RNA editing to generate functional mRNA (Maslov et al., 2019). These features are not always retained across trypanosomatid species.

The divergence in trypanosomatid morphology, transmission, and lifecycle development has facilitated an adaption to a diverse range of hosts and vectors. The different surface protein adaptations of *T. brucei*, *T. cruzi* and *Leishmania* spp. exemplify the variant strategies adopted by these parasites to evade the immune systems of their hosts and vectors. For example, *T. brucei* is extracellular and proliferates in the blood and tissue of mammals. Its cell surface is encoded by a very extensive repertoire of variant surface glycoproteins (VSGs) (Berriman et al., 2005; Wickstead et al., 2004). VSG variation is essential to sustain long-term infections, during which antigenically distinct VSG types dominate at each peak, facilitating host immune evasion (Borst, 2002; Pays et al., 2004). *T. cruzi* is an intracellular parasite of wild and domestic mammals. The nuclear genome contains an expanded family of mucin genes that represent up to 6% of the genome (Buscaglia et al., 2006) and, along with trans-sialidases (Nardy et al., 2016), these genes enable sustained infections. *Leishmania* spp. are intracellular trypanosomatids whose cell surface is covered by a thick layer of glycoconjugates, including families of GP63 major surface proteases (MSPs), also known as leishmanolysin (Yao, 2010).

Studies have largely focused on pathogenic dixenous trypanosomatids, which can hold broad host niches, capable of

Institute of Immunology and Infection Research, School of Biological Sciences, University of Edinburgh, Edinburgh EH9 3FL, UK.

\*Author for correspondence (guy.oldrieve@ed.ac.uk)

© G.R.O., 0000-0003-1428-0608; B.M., 0000-0002-7705-1506; J.L., 0000-0002-0144-2316; K.R.M., 0000-0003-0309-9184

This is an Open Access article distributed under the terms of the Creative Commons Attribution License (<https://creativecommons.org/licenses/by/4.0>), which permits unrestricted use, distribution and reproduction in any medium provided that the original work is properly attributed.

Received 19 January 2022; Accepted 25 March 2022

infecting multiple mammalian species (Funk et al., 2013). In contrast, non-pathogenic dixerous trypanosomes, such as *Trypanosoma theileri* and *Trypanosoma melophagium*, can be highly specific to their host and vector. These species represent an attractive model to study the basis of host and vector specificity. For the remainder of this manuscript, we refer to species that cause no overt pathogenicity in immunocompetent hosts as non-pathogenic. We recognise that 'non-pathogenic' species may still cause slight detriment to their hosts, which is often difficult to detect, especially when prevalence is high in the host population.

*Trypanosoma theileri* is a non-pathogenic bovine parasite which has a reported prevalence of 80% in cattle in the US and Europe when screened via culture-based methods (Farrar and Klei, 1990; Matthews et al., 1979; Mott et al., 2011; Schlafer, 1979). *T. theileri* is transmitted by tabanid flies (Böse and Heister, 1993). It can cause lifelong infections but remains at an extremely low parasitaemia in immunocompetent animals, indicating the presence of an effective host immune evasion mechanism or strict self-imposed population control, which prevents overt disease (Doherty et al., 1993; Seifi, 1995). Experimentally, *T. theileri* can sustain an infection for at least 12 weeks (Mott et al., 2011) which, combined with their non-pathogenic nature, has stimulated development of *T. theileri* as a potential vaccine delivery vehicle (Mott et al., 2011). The genome of *T. theileri* encodes five predicted surface protein families. These are four unique protein families, *T. theileri* putative surface proteins (TTPSPs) and one MSP family (Kelly et al., 2017). Together these genes represent ~9% of the genome of *T. theileri*, comparable to the representation of the VSG gene family in *T. brucei brucei* (TREU927/4) (Berriman et al., 2005). Lastly, the trans-sialidases that characterise *T. cruzi* were also found to be highly expressed in *T. theileri*. These findings led to the suggestion of a novel immune evasion mechanism in *T. theileri*, contrasting with the well-known system in African trypanosomes and distinct from that in *T. cruzi* or *Leishmania* (Kelly et al., 2017). *T. theileri* is at the base of a clade that comprises *Trypanosoma rangeli*, *Trypanosoma cruzi* and *Trypanosoma grayi* (Kelly et al., 2014, 2017), distinct from African trypanosomes, such as *T. brucei*. *T. grayi* is transmitted via the tsetse fly between African crocodylians via ingestion of tsetse faeces containing infective metacyclic forms (Hoare, 1929, 1931).

*Trypanosoma melophagium* is a non-pathogenic trypanosome of the subgenus *megatrypanum*, transmitted between sheep via the sheep ked. This flightless insect vector has been eradicated from much of its original geographic distribution due to widespread pesticide use. However, where the sheep ked persists, it often carries *T. melophagium* (Gibson et al., 2010; Martinković et al., 2012). In a study of organic sheep farms, *T. melophagium* was found to be present in 86% of keds, however, blood smears from sheep on the same farms did not detect trypanosomes (Martinković et al., 2012). Other surveys via blood culture found 7.8% of sheep to be infected with *T. melophagium* (Serpil and Zafer, 2008). It has historically been argued that *T. melophagium* is a monoxenous parasite of the sheep ked and that the mammalian host is obsolete for transmission (Flu, 1908; Porter; Swingle, 1911). However, extensive studies demonstrated a mammalian host is required (Hoare, 1923). Experimental infections of sheep with *T. melophagium* suggested the longest infection lasts 3 months and there is no lasting immunity as sheep can be reinfected with *T. melophagium* after several months of isolation (Gibson et al., 2010; Hoare, 1972).

Molecular markers place *T. melophagium* as a close relative to *T. theileri* (Martinković et al., 2012). SSU rRNA shares ~98% identity between *T. theileri* and *T. melophagium* isolates (Gibson et al., 2010). Presumably the divergence of *T. theileri* and

*T. melophagium* is associated with their discrete host niches (Gibson et al., 2010; Martinković et al., 2012). Nonetheless, *T. theileri* and *T. melophagium* undergo a similar transmission cycle where metacyclic forms are produced in the insect hindgut and the infective forms are then believed to be transmitted to their mammalian host via the mouth, by ingestion of insect faeces or the whole insect body. Trypanosomes then invade their mammalian hosts and proliferate in the blood and, potentially, tissues before being taken up as a bloodmeal by their insect vector (Böse and Heister, 1993; Hoare, 1923).

A notable contrast in the biology of these parasites is the divergence in the life history of their vectors. Sheep keds, which transmit *T. melophagium*, spend their entire life attached to either the skin or wool and hair of sheep. Both male and female keds feed on their mammalian host (Underwood et al., 2015). Tabanids, which transmit *T. theileri*, breed and lay their eggs in soil, water, or trees. The larvae and pupae stages live on vegetation and soil. Only female adults feed on mammalian blood, which is essential for egg production. Although adult tabanids show considerable adaptation to blood feeding, they also feed on the sugars of plants (Chainey, 1993).

Here we derive the *T. melophagium* genome using a combination of long and short read technologies. The genome, and its protein encoding genes, was compared to *T. theileri*, to provide insight into the biological specificity exhibited by each parasite in the context of their close phylogenetic relationship.

## RESULTS

### *T. melophagium* genome assembly

An initial assessment of the *T. melophagium* genome, via k-mer counting, predicted that it was smaller than that of *T. theileri* (22.3 Mb and 27.6 Mb, respectively), this variation being observed in its repeat and unique sequence (Table 1). Notably, both genomes are predicted to have extremely low heterozygosity (0.3 and 0.4 for *T. melophagium* and *T. theileri*, respectively) in comparison to other *Trypanosoma* isolates (Oldrieve et al., 2021). Large gene families, such as the TTPSPs, only account for ~10% of the *T. theileri* genome and so are predicted to have a minor effect in the heterozygosity calculation. The k-mer counting prediction was similar in size to the final assembly (Table 1). The *T. melophagium* assembly consisted of 64 contigs in comparison to 253 for *T. theileri*. BUSCO assessments predict that both assemblies are 100% complete, although *T. theileri* is slightly fragmented (Table 1).

The *T. melophagium* and *T. theileri* genomes were aligned to highlight the conservation of collinearity. The conservation is more similar to the conservation between the species *T. brucei* TREU927/4 and *T. congolense* IL3000 2019 than between isolates of the same species, *T. brucei* TREU927/4 and *T. brucei* Lister 427 2018 (Fig. 1, Fig. S3). The *T. melophagium* genome was annotated with 10,057 protein encoding genes, in comparison to 11,312 in *T. theileri* (Fig. 2C, Table 1) (Kelly et al., 2017).

Kinetoplastid genomes, proteomes and transcriptomes were downloaded from TriTrypDB (Aslett et al., 2010). Proteome completeness was assessed with BUSCO. Those above 85% complete were retained, leaving 44 isolates from 9 genus (File S1). *T. theileri* and *T. melophagium* have some of the smallest genomes in this study and have the lowest GC content (40.1% and 41.2%, respectively), contrasting with the kinetoplastid mean of 48.4% (Fig. 2A).

Environmental temperature (Lao and Forsdyke, 2000; Paz et al., 2004), generation time (Shah and Gilchrist, 2011), neutral drift (Eyrewalker, 1991; Rao et al., 2011), rRNAs (Plotkin et al., 2004), translational accuracy/efficiency (Akashi, 1994; Hu et al., 2013;

**Table 1. Genome assessment**

	<i>T. melophagium</i>	<i>T. theileri</i> (32)
k-mer based genome survey		
Heterozygosity (%)	0.30	0.41
Genome length (Mbp) / Repeat / Unique	22.28 / 4.16 / 18.13	27.62 / 7.97 / 19.65
Genome assembly statistics (for scaffolds longer than 200 bp)		
Number of contigs	64	253
Length (Mbp)	23.3	29.6
Minimum / maximum / mean (bp)	5,186 / 1,230,212 / 364,120	791 / 1,635,300 / 117,005
N50	505,851	517,122
GC (%)	41.2	40.1
Genome BUSCO assessment		
Complete/ single copy/ duplicated/ fragmented	100 / 100 / 0 / 0	99.2 / 99.2 / 0 / 0.8
Annotation		
Number of genes	10,057	11,312
Annotation BUSCO assessment		
Complete/ single copy/ duplicated/ fragmented	100 / 100 / 0 / 0	99.2 / 99.2 / 0 / 0.8

The assemblies used in this assessment represent the final draft of the *T. melophagium* assembly produced during this study and the *T. theileri* assembly available from TriTrypDB (Aslett et al., 2010; Kelly et al., 2017). The k-mer spectra plots associated with the first section of the table are found in Fig. S1.

Shah and Gilchrist, 2011; Sorensen et al., 1989), gene splicing and protein folding (Novoa and de Pouplana, 2012) have all been hypothesised to cause codon bias. However, codon bias can be influenced by nutrient availability (Seward and Kelly, 2016). Species with low nitrogen availability, such as the plant trypanosomatid, *Phytomonas*, have an AT rich genome, potentially to mitigate the lack of nitrogen in their plant hosts (Seward and Kelly, 2016). Selection acting on genome nucleotide cost (Sc) is in competition with selection acting to alter the translational efficiency of the genome (St) (Seward and Kelly, 2016, 2018). Alternative hypotheses for the cause of codon bias can be excluded by analysing

closely related species with similar lifestyles (Seward and Kelly, 2016). Based on universal single copy orthologues, selection pressure acting on the translational efficiency is minimal for both *T. theileri* and *T. melophagium* (Fig. 2B). In contrast, they show the greatest predicted selection pressure acting to reduce the nucleotide cost of any kinetoplastid genome, including the closely related *T. grayi*. The AT biased content can be interpreted as a remodelling of the *T. theileri* and *T. melophagium* genomes to reduce the cost of the genome (Fig. 2A,B). This pattern was consistent when every coding sequence (CDS) was compared (Fig. S4A,B) and in universal single copy orthologs which are essential for every life-cycle stage of

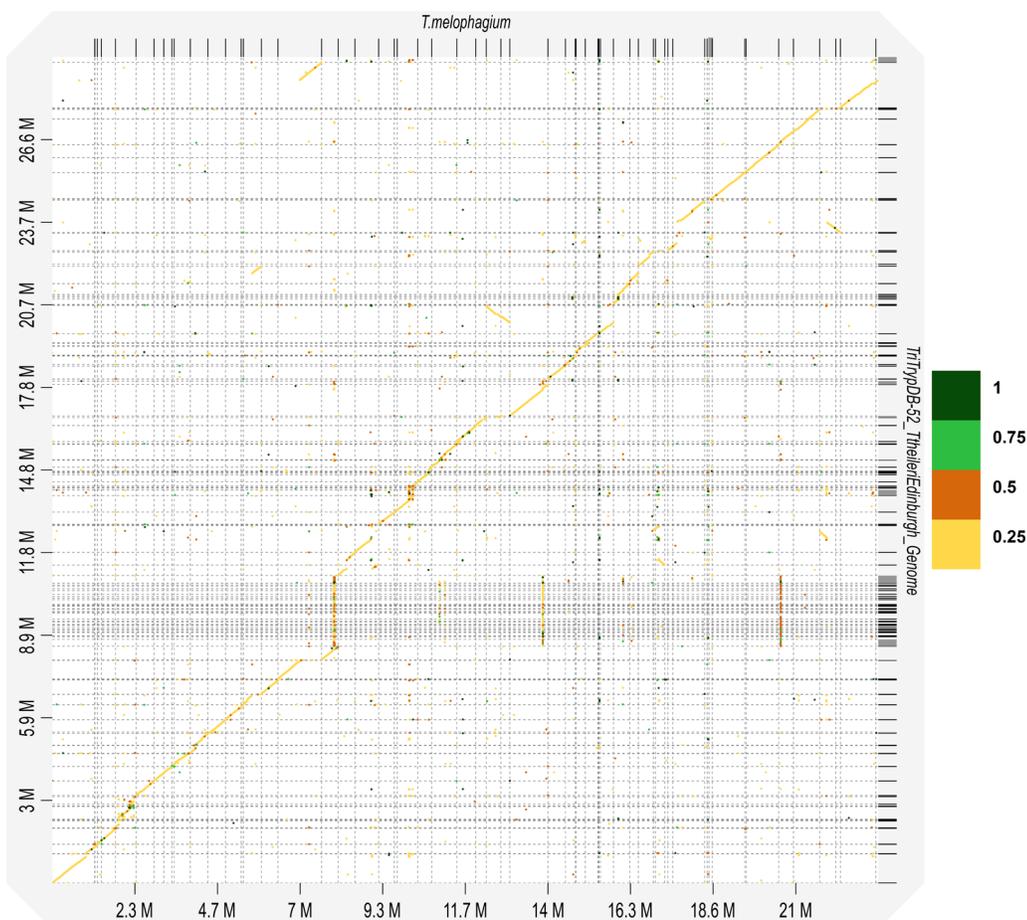


**Fig. 1. Synteny of the *T. melophagium* and *T. theileri* genome sequences highlights conservation and identity between the two species.** The legend refers to the percentage identity between the sequences.

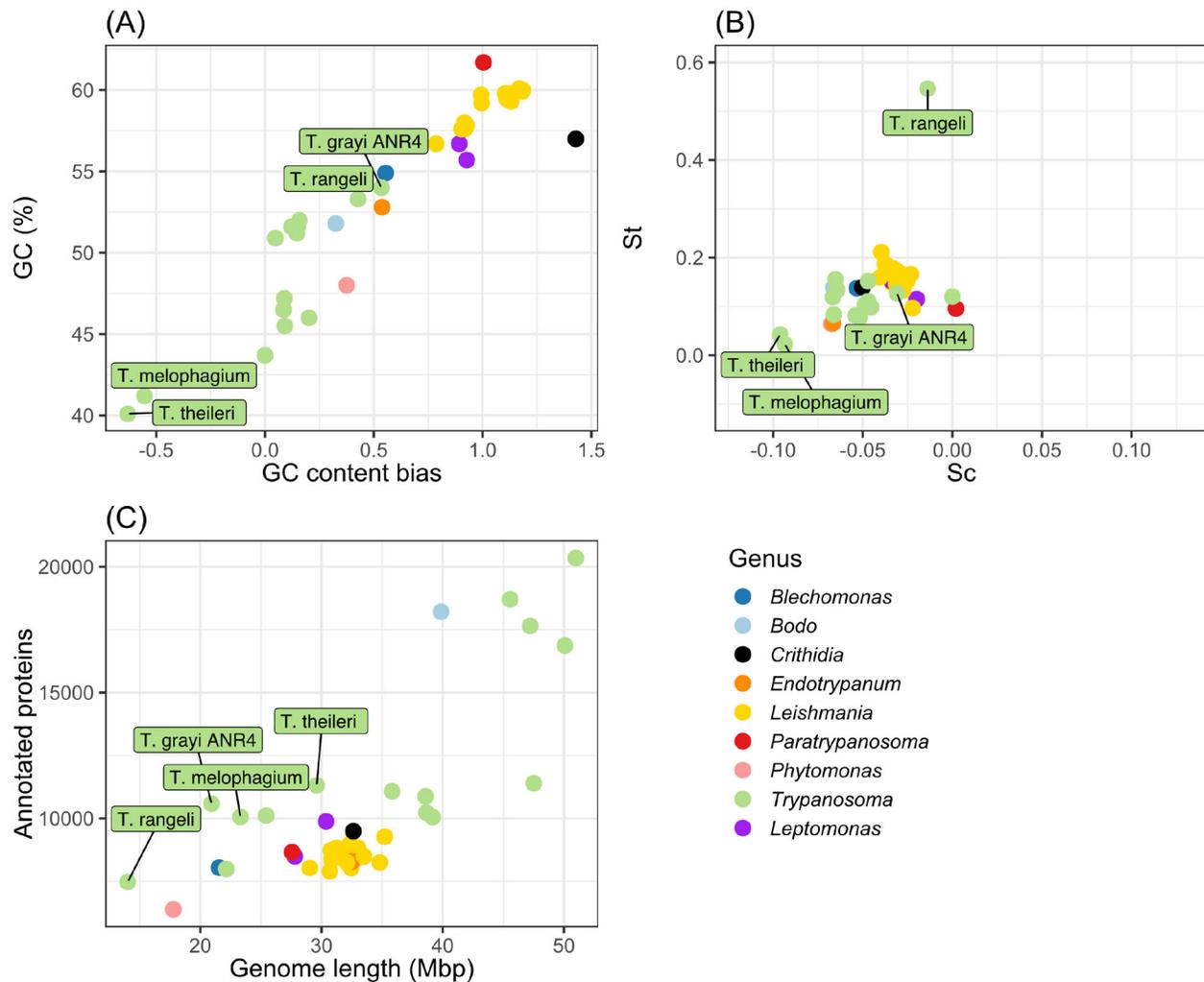


**Fig. 2. Kinetoplastid genome comparison.** (A) GC content across the whole genome and GC content bias in the CDS of kinetoplastid universal single copy orthologues ( $n=992$ ). GC content (GC) $>0$ =GC content bias. GC  $<0$ =AT content bias. (B) Selection acting on translational efficiency (St) and selection acting on nucleotide cost (Sc) in kinetoplastid universal single copy orthologues. Sc  $>0$ =Selection acting to increase codon nucleotide cost. Sc  $<0$ =Selection is acting to decrease codon nucleotide cost. St  $>0$ =Selection is acting to increase codon translational efficiency. St  $<0$ =Selection acting to decrease codon translational efficiency. (C) Counts of annotated protein sequences of publicly available kinetoplastids compared by genome size.

*T. brucei* (Fig. S4C,D). *T. rangeli* displays the highest level of selection pressure acting to increase translational efficiency (Fig. 2B), potentially linked to its reduced genome length (Fig. 2C).

#### Orthologous protein clustering and phylogenetic inference

Orthologous clustering identified genes that descended from a gene in the last common ancestor of the 44 kinetoplastid proteomes used in this study (Fig. 2, File S1). From the 44 proteomes, 18,274 orthogroups were identified (96.5% of the proteins used in this study were included in one of these orthogroups), 992 orthogroups were single copy and contained all isolates.

A species tree was generated as part of the orthologous protein clustering. Using genetic markers, previous studies have noted the similarity between *T. melophagium* and *T. theileri* (Gibson et al., 2010; Martinković et al., 2012). Based on 2,312 gene trees, *T. theileri* is the closest isolate to *T. melophagium* and groups with the stercorarian trypanosomes, which include *T. cruzi*, *T. grayi* and *T. rangeli*, rather than with salivarian trypanosomes such as *T. brucei* (Fig. 3). *T. grayi* is the closest isolate to the *T. melophagium* and *T. theileri* clade and is closer in size to the genome length of

*T. melophagium* than to *T. theileri* (Fig. 2C). *T. melophagium* and *T. theileri* are closely related species with relatively short branch lengths (0.093 and 0.088 substitutions per site, respectively). In comparison, *T. congolense* is more divergent from *T. brucei* (0.249) whilst the isolates within *T. brucei* (*T. brucei brucei* Lister 427 2018:0.0009, *T. brucei evansi* STIB805: 0.003, *T. brucei brucei* TREU927/4: 0.003 and *T. brucei gambiense* DAL972:0.004) show less divergence than seen between *T. theileri* and *T. melophagium*.

*T. theileri* has a greater number of species-specific orthogroups than *T. melophagium* and 12.9% of its genes are assigned to one of these orthogroups, while *T. melophagium* has only 2.7% of its genes in a species specific orthogroup (Table 2). Terminal branch length is correlated with specific orthogroup counts, which could account for the discrepancy. However, *T. melophagium* and *T. theileri* are each other's most recent common ancestor and have been evolving at a roughly similar rate since this time, with similar terminal branch lengths (Fig. 3). To visualise these differences, the number of genes in each orthogroup was compared between *T. melophagium* and *T. theileri*. Orthogroups associated with host interaction protein families were highlighted based on their identification as a putative

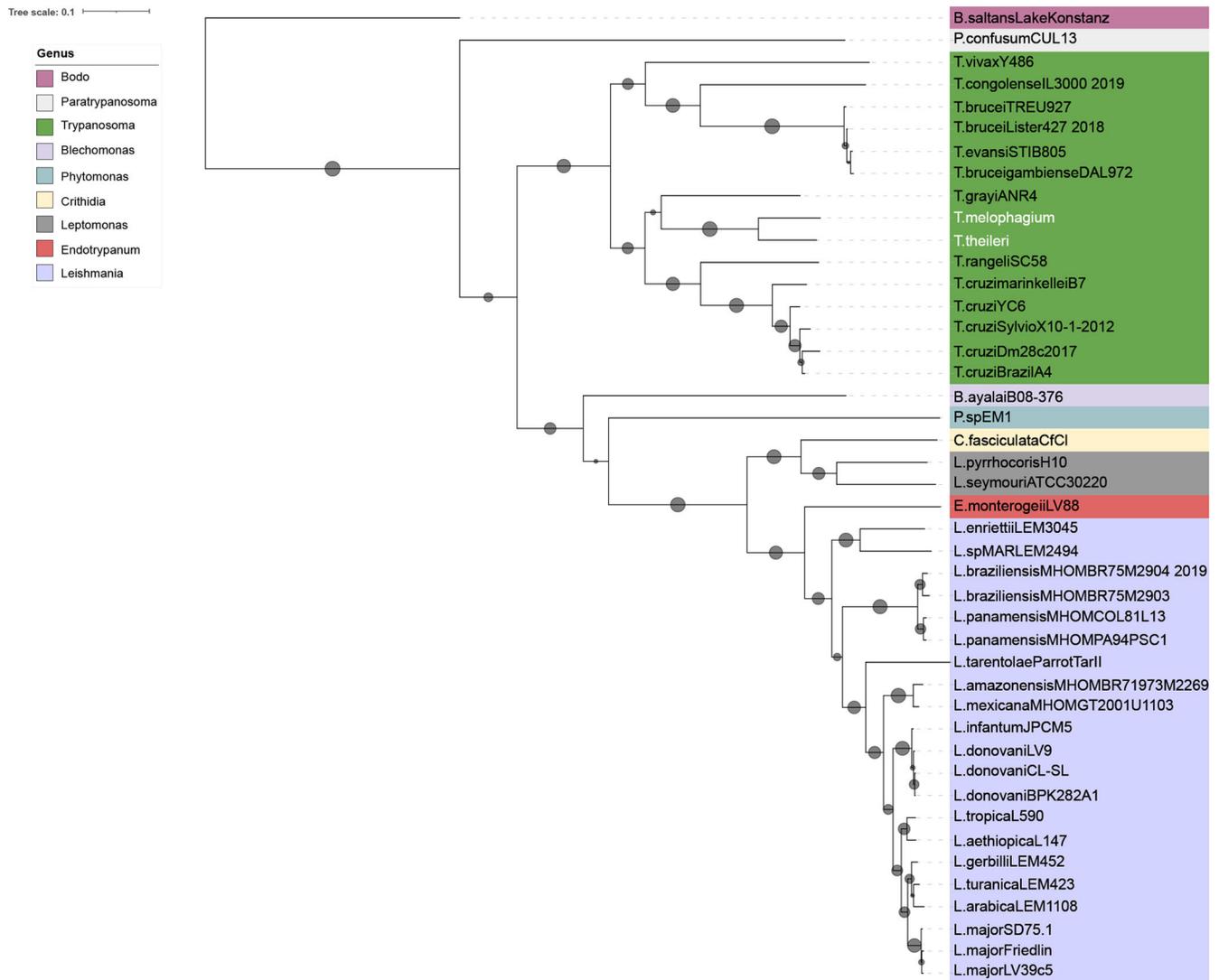


**Fig. 3. Species consensus tree based on 2,312 gene trees created by STAG and STRIDE, OrthoFinder.** The support values are represented by circles. Support values correlate to the proportion of times that the bipartition is seen in each of the individual trees used to create the consensus tree. The scale represents substitutions per site.

cell surface protein by Kelly et al. (2017). Many of the *T. theileri* species specific orthogroups expansions belong to a cell surface family (Fig. 4A).

### Interaction with the mammalian host and predicted cell surface proteins

Firstly, and as expected, *T. melophagium* was found to lack any genes in orthogroups which contained VSGs, characteristic of African trypanosomes (File S4). To validate this, a blast search was

**Table 2. Orthologous protein clustering statistics of *T. melophagium* and *T. theileri***

	<i>T. melophagium</i>	<i>T. theileri</i>
Number of genes	10,057	11,312
Genes in orthogroups (%)	97.3	97.4
Orthogroups containing species (%)	43.9	44.2
Number of species-specific orthogroups	76	121
Genes in species-specific orthogroups (%)	2.7	12.9
Comparatively expanded orthogroups	787	563

The full species-specific clustering summary can be found in File S3.

performed using a relaxed cut off ( $1e-5$ ) using the *T. melophagium* genome as the database and *T. brucei* TREU927/4 VSGs as the query. No hits were identified.

To enable comparison to the *T. theileri* genome analysis, the genes and orthogroups from this study were annotated with the host interaction genes from Kelly et al. (2017). Across the entire genome, *T. theileri* is predicted to contain 1,265 more genes than *T. melophagium* (Table 2). Examination of orthogroups which were associated with a *T. theileri* putative surface protein (TTPSP) revealed a large expansion in *T. theileri* (1,251 genes) compared to *T. melophagium* (10 genes) which could equate to much of the disparity in genome size (Fig. 4). To confirm the difference in TTPSPs, the *T. theileri* transcripts were subjected to a blastn search against a database consisting of the *T. melophagium* transcripts ( $1e-25$  cut-off). The *T. melophagium* transcripts were derived from the genome annotation analysis. Only nine *T. theileri* TTPSPs aligned to *T. melophagium*.

TTPSPs were split between four orthogroups in the original *T. theileri* genome analysis but were split between 66 orthogroups in this analysis (Table 3) (Kelly et al., 2017). TTPSPs share conserved

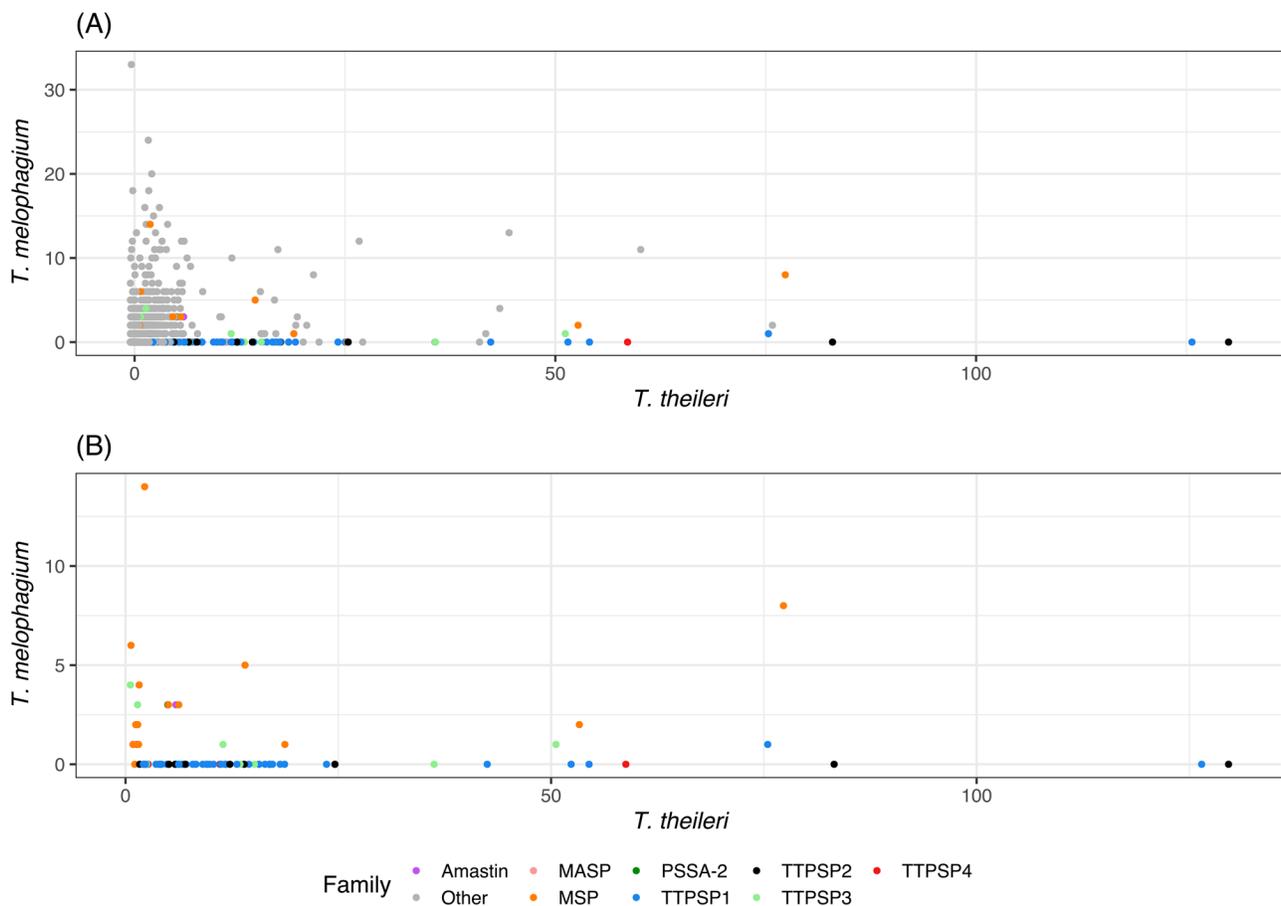


**Fig. 4. (A) All orthogroups and (B) orthogroups associated with host interaction size comparison between *T. melophagium* and *T. theileri*.** Each dot represents the numbers of genes found in each orthogroup for both species. The orthogroups have been annotated with their designation as either a putative cell surface protein family or 'other' (Kelly et al., 2017).

C terminal GPI addition and N terminal signal sequences and contain regions of high divergence in the remainder of the sequence. TTPSPs are highly expressed as a family at the population level and are largely contained within tandem arrays, highlighting a similarity to the VSGs of *T. brucei* (Kelly et al., 2017). Excluding *T. melophagium*, TTPSPs are absent from all other kinetoplastid species analysed (File S4) revealing their specific innovation in these related trypanosomatids.

Following the TTPSPs, the largest expanded gene family in *T. theileri* are the MSPs. This protein family belongs to the peptidase M8 family of metalloproteinases. MSPs are likely to have contrasting roles in different life stages but their best understood function is to bind and cleave members of the complement system and for evasion of other cellular and antimicrobial immune defences

(Yao, 2010). This role presumably allows for evasion of complement-mediated proteolysis and therefore assists survival in the insect and mammalian hosts (Yao, 2010). Orthogroups which annotated as MSPs were expanded in *T. melophagium*, such as OG0008865. *T. melophagium* also has a species specific orthogroup (OG0009903) consisting of 11 proteins and annotated as MSP. Combined, these results suggest that the surface protein environment of *T. melophagium* and *T. theileri* are distinct and that genes encoding these proteins account for most of the discrepancy in the genome sizes.

#### Clade and species specific orthogroups

*T. grayi*, *T. melophagium* and *T. theileri* contain 42 clade-specific orthogroups including the MSP orthogroups OG0000590 and

**Table 3. Cell surface orthogroup counts from Kelly et al. (2017) (32) and this study along with counts of genes present in each category**

Cell surface conservation	Annotation	Orthogroup count		Gene count	
		Kelly et al., 2017	This study	<i>T. theileri</i>	<i>T. melophagium</i>
Conserved	Amastin	1	2	7	4
Conserved	MASP	1	1	1	1
Conserved	MSP	1	18	229	52
Conserved	PSSA-2	1	1	5	3
Unique	TTPSP1	1	42	720	1
Unique	TTPSP2	1	10	301	0
Unique	TTPSP3	1	11	157	9
Unique	TTPSP4	1	3	73	0

OG0008095. Both MSP orthogroups were expanded in *T. theileri* in comparison to *T. grayi* and *T. melophagium*. *T. melophagium* and *T. theileri* share 81 orthogroups specific to the two species. Twelve of the orthogroups are putative cell surface protein families, including five representatives from TTPSP and seven MSP orthogroups. Of the nine remaining annotated orthogroups, OG0008096 is the largest and contains trans-sialidases. The orthogroup is expanded in *T. theileri* ( $n=17$ ) compared to *T. melophagium* ( $n=5$ ).

*T. theileri* has 121 species specific orthogroups. Sixty-four of these were putative host interaction genes (Kelly et al., 2017). Two annotated orthogroups remained, which included a leucine-rich repeat family associated with protein binding (OG0011868) and a calpain cysteine protease family (OG0018204). *T. melophagium* has 76 species-specific orthogroups, 68 of these were unannotated. MSP families were annotated in three of the remaining orthogroups (OG0009903, OG0013746 and OG0013747). Other annotated species-specific orthogroups consisted of an actin family (OG0018163) along with several families associated with protein binding, WD domain G-beta repeat (OG0018131) and a leucine rich repeat family (OG0018098).

### Cell surface modifying enzymes

Trans-sialidases are differentially expanded in *T. theileri* and *T. melophagium*, with 38 and eight genes, respectively. Of the four orthogroups containing trans-sialidase, two do not contain proteins from *T. melophagium* (OG0011818 and OG0015016). These two orthogroups contain proteins from *T. cruzi* and so are likely to have been lost by *T. melophagium* and *T. grayi*. In *T. cruzi*, trans-sialidases are involved in host immune evasion (Nardy et al., 2016).

Invertases are typical of the cell surface of *Leishmania* and are thought to transform sucrose into hexose in the gut of the vector. The orthogroups (OG0000150 and OG0000409) that include 20 *T. theileri* invertase genes only have three members in *T. melophagium* and three members in *T. grayi*. This expansion might indicate an adaptation of *T. theileri* to its vector, the tabanid fly, which can feed on sugary flower nectar (Kniepert, 1980). In contrast, the *T. melophagium* vector, the sheep ked, exclusively feeds on mammalian blood. The orthogroups which contain the *T. theileri* invertase genes (OG0000150 and OG0000409) contain only one gene from the plant parasite *Phytomonas* (Jaskowska et al., 2015; Sanchez-Moreno et al., 1992), suggesting a different mechanism for sucrose metabolism in these parasites.

Other putative cell surface modifying molecules, such as UDP-galactose/UDP-N-acetylglucosamine transferases (OG0000001) were expanded in *T. theileri* ( $n=60$ ) compared to *T. melophagium* ( $n=11$ ).

### Glycolysis

Kelly et al. (2017) compared *T. brucei* and *T. theileri* transcriptomes which revealed differences in the abundance of glycosomal enzyme mRNAs. Particularly, pyruvate orthophosphate dikinase, phosphoenolpyruvate carboxykinase and malate dehydrogenase were found to be >10 fold more abundant in *T. theileri* than in *T. brucei* (Kelly et al., 2017). We confirm that enzymes associated with the glycolytic pathway are present in *T. melophagium* (File S4) and found that *T. melophagium* has expanded the orthogroups associated with three glycolytic enzymes. These included pyruvate orthophosphate dikinase (OG0000570), phosphoenolpyruvate carboxykinase (OG0000120) and malate dehydrogenase (OG0000332), whilst *T. melophagium* has a reduced number of genes in the fumarate reductase orthogroup (OG0000078).

Orthogroups associated with peroxisome targeting were found to be in equal numbers (OG0004108 PEX5 and OG0003998 – PEX7). All other glycolytic enzymes are present in equal numbers in the two species. Therefore, it is likely that the glycolysis pathway is conserved in *T. melophagium*.

### Life cycle

Extensive studies of *T. brucei* have identified genes which are associated with key stages of the *T. brucei* life cycle. These studies tracked genes associated with stumpy formation in the blood stream form (Cayla et al., 2020; Ling et al., 2011; Liu et al., 2020; Mony et al., 2014) and regulators of metacyclogenesis (Toh et al., 2021). These genes were combined with a list of validated development associated genes such as the RNA binding proteins RBP6, RBP7, RBP10 and ZFP2 and ZFP3 along with developmental regulators NRK A, NRK B, RDK1, RDK2, MAPK2 and phosphatases such as PTP1 and PIP39 (Domingo-Sananes et al., 2015; Gale et al., 1994; Gale and Parsons, 1993; Jones et al., 2014 a; Müller et al., 2002; Szöör et al., 2010, 2006; Walrad et al., 2009). Most of the orthogroups containing these genes were represented with a similar number of genes in each species, indicating the presence of an environmental sensing ability and developmental competence (Fig. 5). However, there were notable differences. There is an expansion in the orthogroups containing KRIPP14, which is a mitochondrial SSU component (Mony et al., 2014), in *T. theileri*. *T. melophagium* has expanded its orthogroups containing the kinases NRK (Domingo-Sananes et al., 2015; Gale et al., 1994), NEK and (Gale and Parsons, 1993) ADKF (Mony et al., 2014) along with a dual specificity phosphatase (DsPho) and protein phosphatases 1 (PP1) (Mony et al., 2014; Mony and Matthews, 2015). Both *T. theileri* and *T. melophagium* are missing metacaspase (MCA1) which is associated with the later stages of progression towards metacyclic forms in *T. brucei* (Toh et al., 2021) and Hyp12, which upregulates bound mRNAs during development based on tethering assays in *T. brucei* (Erben et al., 2014; Lueong et al., 2016; Mony et al., 2014; Mony and Matthews, 2015). Puf11, an effector molecule required for kinetoplast repositioning in epimastigotes (Toh et al., 2021), is also absent in *T. melophagium*.

Life-cycle regulatory genes and genes controlling meiosis SPO11, MND1, HOP1 and DMC1, along with the cell fusion protein HAP2/GCS1 (Peacock et al., 2021), were found in *T. melophagium* and *T. theileri* (Fig. 5), suggesting maintenance of a sexual stage.

### RNA interference and transposable elements

All five core genes that represent the trypanosome RNAi machinery (AGO1, DCL1, DCL2, RIF4 and RIF5) were present in *T. melophagium*, with an extra gene in the orthogroup containing DLC2 (File S4). Therefore, a functional gene silencing pathway is likely to be present in *T. melophagium*, matching the prediction in *T. theileri*.

Retrotransposon counts highlighted an expansion in *T. cruzi* and *T. vivax* isolates, along with *T. brucei* Lister 427 2018 (Fig. S5A, File S1). *T. melophagium* and *T. theileri* have not expanded their retrotransposon repertoire. A similar pattern was observed for long terminal repeat (LTR) retrotransposon counts, which show a positive correlation with genome size (Fig. S5B).

### DISCUSSION

*T. melophagium* and *T. theileri* are closely related trypanosomes that have distinct hosts and vectors (Gibson et al., 2010; Martinković et al., 2012). Here, the genome of *T. melophagium* was sequenced

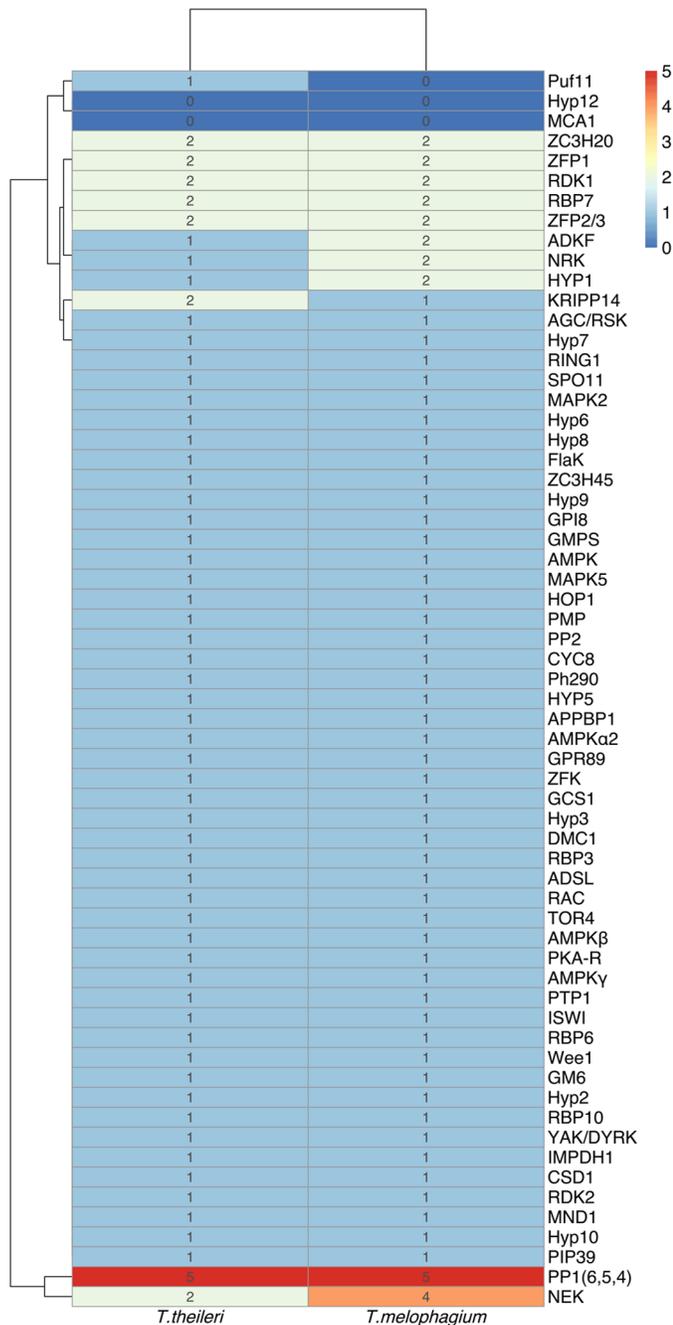


**Fig. 5. Genes associated with development, and related proteins, at various stages throughout the *T. brucei* life cycle.** The number of genes in orthogroups associated with developmental regulation have been quantified in *T. theileri* and *T. melophagium*.

and a draft assembly was produced and annotated. The annotated proteome was incorporated into a comparison with *T. theileri*, and other publicly available kinetoplastid proteomes, to determine their phylogenetic relationship and to explore the genomic basis of the host and vector specificity of these non-pathogenic trypanosomatids.

Although the two genomes compared in this analysis are predicted to be complete (Table 1), their assembly and annotation were performed 5 years apart using different assembly pipelines and sequencing technologies. Comparing assemblies obtained using the same sequencing technologies and assembly pipelines would allow

for greater confidence in the observed variations in their genome content as updated methods and long-read sequencing continue to improve the quality of genome assemblies and, therefore, completeness. This was not possible since many of the assembly tools used are specific for the sequencing technologies whilst there has been substantial development in assembly methods between the two studies. However, based on the convergence of the k-mer counting based prediction with the assembly sizes, along with 100% complete BUSCO scores, we were reassured by the quality of the draft assemblies and the subsequent comparisons of their genome content.

Using k-mer counting based predictions, *T. melophagium* was anticipated to have a smaller genome than *T. theileri*. This held true when the data were assembled (Table 1). The *T. melophagium* genome is more similar in size to *T. grayi*, the closest relative to *T. melophagium* and *T. theileri*, than to *T. theileri* (Figs 2 and 3). *T. theileri* has likely expanded its genome size since speciation occurred. A peculiarity of the *T. theileri* and *T. melophagium* isolates analysed in this study is their highly reduced heterozygosity, in contrast to African trypanosomes (Oldrieve et al., 2021). Whilst only one genome is available for both species, should these isolates represent the species as a whole, the reduced heterozygosity could be linked to a founder effect (Pool and Nielsen, 2007). As *T. theileri* and *T. melophagium* have specific host and vector niches, the small population that initially expanded into the niches possibly underwent a significant population bottleneck, especially as host domestication caused eradication of wild progenitors and wild relatives, which could have facilitated a reduction in heterozygosity, induced by genetic drift. Alternatively, the absence of a sexual cycle could contribute to the reduced heterozygosity. Although *T. melophagium* and *T. theileri* contain genes required for meiosis, this does not confirm the species undergo sexual reproduction.

Selection appears to be acting to reduce the genome wide nucleotide biosynthesis cost in both *T. theileri* and *T. melophagium* (Fig. 2B) which has remodelled their genomes toward an AT bias, contrasting with all other kinetoplastid genomes analysed in this study (Fig. 2A,C). The predicted selection pressure acting to reduce nucleotide cost is at the expense of translational efficiency (Fig. 2C) and is greater than for the free-living *Bodo saltans*, or monoxenous insect parasites such as the early-branching *Paratrypanosoma confusum* and *Phytomonas* EM1. *Phytomonas* has limited access to nitrogen as it infects nitrogen deficient plants and has been highlighted as an example where diet can cause selection to reduce the species genome nucleotide cost, through a reduction in GC content (Seward and Kelly, 2016). We propose that the reduction in the selection cost of *T. theileri* and *T. melophagium* may be related to their non-pathogenic nature. By remodelling their genome to an AT bias, they may have reduced their cost to their host, facilitating reduced pathogenicity. Closely related species of bacteria exist on a spectrum from pathogen to symbiont, highlighting how a selective advantage can arise from a parasite reducing the cost to its host (Toft and Andersson, 2010). It is possible that *T. melophagium* and *T. theileri* are part of a similar spectrum amongst trypanosomatids. We acknowledge that alternative hypotheses exist for the reduced nucleotide cost associated with the AT rich genome, such as tissue niche adaptation in their mammalian host or selection primarily operating within the arthropod vector rather than mammalian host.

This clade-specific genome remodelling provides an example of the similarity between *T. theileri* and *T. melophagium*. However, the species have contrasting hosts, vectors, and genome sizes. Genome annotation and orthology inference identified candidates for their discrepancy in genome size. When species specific orthogroups

were compared, the greatest contrast was between orthogroups associated with the putative cell surface, with the largest expansions detected in *T. theileri* being of TTPSP and MSP surface protein families (Fig. 4). Although both species undergo a cyclical transmission cycle, which includes mammalian and insect stages, we hypothesise the respective prevalence in their mammalian hosts, and the contrasting life history of their respective vectors could explain the genome expansion in *T. theileri*. *T. theileri*, spread by tabanids, are found in over 80% of livestock (Farrar and Klei, 1990; Matthews et al., 1979; Mott et al., 2011; Schlafer, 1979). In comparison, *T. melophagium* exhibits lower detected prevalence, being rarely identified in its mammalian host via blood smears (Martinković et al., 2012) or after blood culture (Serpil and Zafer, 2008). Moreover, sheep keds, which transmit *T. melophagium*, are intimately associated with their mammalian host, spending their entire life either on the sheep's skin or wool. Here, males and females feed solely on mammalian blood providing many opportunities for transmission of *T. melophagium* from the sheep to the sheep ked (Hoare, 1923). Therefore, there is potentially less advantage for *T. melophagium* to invest in mammalian immune evasion mechanisms required to extend the length of its infection in sheep, since it has many transmission opportunities. The limited investment in *T. melophagium* is emphasised by their relatively unsophisticated putative TTPSP-related repertoire alongside modestly expanded species-specific MSP families (Fig. 4). Instead, *T. melophagium* could rely on its ancestral ability to sustain infections in invertebrate hosts, which, although able to be primed to defend against a specific pathogen, rely upon an innate immune response (Cooper and Eleftherianos, 2017).

In contrast, *T. theileri* has a transient host-vector interaction. Tabanid flies of either gender survive on plant sugars, while adult females occasionally feed on mammalian blood (Chainey, 1993). Therefore, potentially *T. theileri* requires extended survival in its mammalian host to sustain transmission between cattle, compared to the intimate long-term association of sheep keds with *T. melophagium*. The investment from *T. theileri* in an expanded surface protein repertoire is likely to support adaptive immune evasion and prolonged survival in the mammalian stage of its life cycle. Alternatively, or additionally, differences between the bovine and ovine immune responses could contribute (Wang et al., 2013). It should be noted that both *T. melophagium* and *T. theileri* prevalence was surveyed via blood smear or blood culture. Although this is a standard approach, studies have highlighted the prevalence of *T. brucei* in adipose tissue (Trindade et al., 2016) and we cannot exclude one species preferentially infecting these tissues, rather than the bloodstream.

Many of the gene families identified in *T. theileri* (Kelly et al., 2017) were divided into multiple orthogroups in this study. The discrepancy is likely to be explained by evolution of the methods used by OrthoFinder. At the time of publication of the *T. theileri* study, OrthoFinder v.1 was available, while our analysis used version v.2.5. For instance, OrthoFinder v.2.5 uses updated sequence alignment tools, such as DIAMOND ultra-sensitive. For this reason, we can speculate that the clustering in this study is more refined, such that the TTPSP families should be divided into smaller protein families. However, large paralogous orthogroups remain the toughest challenge for orthogroup clustering software and so the relationships between this set of proteins will likely continue to evolve alongside the software (Emms and Kelly, 2020).

Genes involved in the trypanosome life cycle, cellular quiescence and meiosis were all detected in *T. melophagium*, suggesting a competent developmental cycle along with the machinery for sexual

recombination. There is an expansion of the *T. theileri* invertase orthogroup which was not present in *T. melophagium*. This is potentially associated with the use of sucrose in the tabanid fly's diet. Although the glycolysis pathway is present in *T. melophagium*, there was an expansion in the pyruvate orthophosphate dikinase, phosphoenolpyruvate carboxykinase and malate dehydrogenase orthogroups. These genes are associated with the branch of the glycolysis pathway that converts pyruvate to succinate to facilitate the recovery of NAD<sup>+</sup> (Kelly et al., 2017). This branch of the glycolytic pathway was upregulated in *T. theileri* in contrast to *T. brucei* (Kelly et al., 2017). Interestingly, the core RNAi genes were detected in *T. melophagium*, consistent with *T. theileri* but distinct from *T. cruzi* which is also a sterocorarian trypanosome, but which lacks the requisite molecular machinery (Ullu et al., 2004).

In summary, we have found that *T. theileri* and *T. melophagium* are closely related species that display substantial remodelling of their genomes to facilitate a reduction in their nucleotide costs, which might reduce the costs they impose on their hosts. *T. theileri* displays a considerable genome expansion, which is associated with a large repertoire of unique proteins that characterise its cell-surface and host-interaction gene repertoire. These genes could facilitate a lifelong infection in its mammalian host. In contrast, the comparatively unsophisticated immune evasion repertoire displayed by *T. melophagium* suggests more limited adaptation to its mammalian host.

## MATERIALS AND METHODS

### Trypanosome culture, DNA/RNA extraction and sequencing

The full list of tools used in this study, and the options used to run those tools, can be found in Table S1.

*T. melophagium* was isolated from sheep blood collected on the island of St Kilda, Scotland, UK (kindly provided by Professor Josephine Pemberton, University of Edinburgh). Whole blood was collected into heparinized vacutainers and used within 2 days. 1 ml of blood was diluted with 5 volumes of a 50% mix of HMI9 supplemented with 20% fetal bovine serum (FBS) and Madin-Darby bovine kidney (MDBK) conditioned medium. All cultures were kept at 37°C and were examined microscopically every 3 days for 6 weeks. After propagation of *T. melophagium* by culturing of the blood sample, the specimens were transferred and co-cultured with fibroblast-like primary cells as feeder cells, isolated from the same blood sample. Due to the short lifespan of these primary cultured cells, *T. melophagium* was subsequently co-cultivated with MDBK cells and then progressively adapted to axenic conditions with a 50% mix of HMI9 and MDBK conditioned medium.

DNA was extracted from cultured *T. melophagium* using a MagAttract high molecular weight DNA kit, following the manufacturer's instructions (Qiagen) and cleaned via ethanol precipitation. The DNA was sequenced with Oxford Nanopore Technology's (ONT) MinION (R9.4.1), following the ONT Rapid Sequencing protocol. Base-calling was performed in high accuracy mode using Guppy (available at <https://community.nanoporetech.com/>) which produced 1.059 gigabases (Gb) of data. PycoQC was used to visualise the data (Leger and Leonardi, 2019). The same DNA was sequenced with BGI's DNBseq (4.201Gb, 150 base pair reads). RNA was extracted with the RNeasy mini kit (Qiagen) including a DNase step, following the manufacturer's instructions and sequenced with BGI's DNBseq (5.019Gb, 100 bp reads). Raw DNA and RNA DNBseq reads were trimmed with Trimmomatic (Bolger et al., 2014).

*T. theileri* sequencing data was downloaded from NCBI. 170 bp genomic reads were used (SRR13482812).

### *T. melophagium* genome assembly and annotation

Jellyfish and GenomeScope were used to provide a k-mer based estimate of the genome size and heterozygosity using the short DNA reads described above (Marçais and Kingsford, 2011; Vurture et al., 2017).

ONT long reads were assembled using Wtdbg2 (Ruan and Li, 2020). For the polishing steps, BWA-MEM (Li, 2013 preprint) was used to align short reads and Minimap2 (Li, 2018) was used to align ONT reads. ONT reads were aligned to the Wtdbg2 draft assembly and three iterations of Racon (Vaser et al., 2017) followed by one round of Medaka (available at <https://github.com/nanoporetech/medaka>) were performed. DNBseq reads were mapped to the Medaka polished assembly, and two iterations of Racon were performed. Short and long reads were aligned to the Racon polished assembly to complete two final iterations of polishing with Pilon (Walker et al., 2014). At each stage of polishing, the quality of the draft genome was assessed using scaffold\_stats.pl (available at <https://github.com/sujaikumar/assemblage>) and BUSCO (Seppey et al., 2019). BUSCO provides a metric for genome assembly and annotation completeness, based on the presence of near-universal single-copy orthologues in a genome assembly or the corresponding annotated proteins.

Both sets of reads were mapped to the draft assembly. Each contig was subjected to a DIAMOND blastx search against the InterProScan database (Buchfink et al., 2015; Jones et al., 2014b). The resulting alignments and DIAMOND hits were visualised with BlobTools (Laetsch and Blaxter, 2017b). Every contig had a DIAMOND hit to sequences from the *Trypanosoma* genus. Therefore, the assembly was confirmed to be free from contamination. However, two contigs were outliers in comparison to the rest of the assembly at under 100x coverage and consisting of only 3,975 and 1,892 base pairs (Fig. S2A). These contigs were removed from the assembly. BUSCO and BlobTools were re-run on this trimmed assembly to assess the final assembly's completeness and coverage (Fig. S2B).

Repeat sequences in the genome were identified and soft-masked using RepeatModeler2 and RepeatMasker (Flynn et al., 2020). BRAKER2 was used to annotate the soft-masked genome in ETP mode. The OrthoDB v10 protozoa database was utilised for protein hints (Kriventseva et al., 2019) with the addition of the *T. theileri* proteome and *T. melophagium* RNAseq evidence (Barnett et al., 2011; Bruna et al., 2021, 2020; Buchfink et al., 2015; Gotoh, 2008; Hoff et al., 2016, 2019; Iwata and Gotoh, 2012; Li et al., 2009; Lomsadze et al., 2014; Stanke et al., 2008, 2006). BRAKER2 produced the protein and transcript files used in the following analysis. The *T. melophagium* proteome was functionally annotated using InterProScan (Jones et al., 2014b) using the Pfam and SignalP databases (Mistry et al., 2021; Nielsen, 2017). Genome conservation of collinearity was compared using D-Genies (Cabanettes and Klopp, 2018).

Publicly available genomes, transcriptomes and proteomes were accessed from TriTrypDB (Aslett et al., 2010) along with the *Phytomonas* EM1 assembly which was accessed from NCBI (Leinonen et al., 2011). The quality of the proteomes were assessed using BUSCO; only isolates which had >85% complete proteomes were included, which left 43 isolates along with *T. melophagium*. A list of all the isolates used in this study can be found in File S1. The assembly statistics of the 44 genomes were assessed using scaffold\_stats.pl (available at <https://github.com/sujaikumar/assemblage>).

The genomes from each of these kinetoplastid isolates were screened for transfer RNA genes using tRNAscan-SE (Chan et al., 2021). The outputs of these results were used to infer the strength of selection acting on translational efficiency and nucleotide cost for each isolate, along with the background mutation bias, using CodonMuSe (Seward and Kelly, 2016, 2018). Each isolate was assessed using (1) every CDS, (2) single-copy universal orthologs (identified in the orthologous protein clustering steps below) ( $n=992$ ) and (3) single-copy universal orthologs, which are essential for every stage of the *T. brucei* life cycle ( $n=158$ ). The last list of genes were identified by screening the universal single-copy orthologs for genes that had a significant reduction in transcript levels in every library of an RNAi phenotype screen (>1.5 log fold decrease) (Alsford et al., 2011).

Each kinetoplastid genome was also screened for retrotransposons and long terminal repeat (LTR) retrotransposons using TransposonPSI (available at <http://transposonpsi.sourceforge.net>) and LTR-harvest (Ellinghaus et al., 2008), respectively.

### Orthology inference

Orthologous proteins from 44 kinetoplastid proteomes were identified with OrthoFinder (Emms and Kelly, 2019) and protein clusters were summarised with KinFin (Laetsch and Blaxter, 2017a), using InterProScan annotations

based on the Pfam and signalP databases (Jones et al., 2014b; Mistry et al., 2021; Nielsen, 2017). A minimal cut-off threshold was not applied to the orthogroup annotation. The orthogroup annotation summary can be found in File S2. A species tree was produced by STAG and STRIDE, as part of the OrthoFinder analysis (Emms and Kelly, 2017, 2018), which was visualised with iTOL (Letunic and Bork, 2007). STRIDE identified *Bodo saltans* as the best root for the consensus species tree.

To confirm the absence of VSGs in *T. melophagium*, all CDS sequences labelled as 'VSG' in the *T. brucei* TREU927/4 reference genome were downloaded from TriTrypDB. A blastn search was performed using these VSG sequences as the query and the *T. melophagium* genome as the database using a loose cut-off (e-value=1e-5). A similar search was performed to confirm the reduced TTPSP counts in *T. melophagium*. For this, the *T. theileri* transcripts were used to query a database made from the *T. melophagium* transcripts (e-value=1e-25).

The cell surface orthogroups in this study were annotated with the orthogroups from Kelly et al. (2017) based on the orthogroup membership of genes in the two analyses. Unless stated otherwise, all of the figures in this study were plotted in R (Team, 2019) using ggplot2 (available at <http://ggplot2.tidyverse.org>) and ggrepel (available at <http://github.com/slowkow/ggrepel>).

### Acknowledgements

We thank Steve Kelly (University of Oxford) for his comments and insights on the manuscript.

### Competing interests

The authors declare no competing or financial interests.

### Author contributions

Conceptualization: G.O., K.M.; Methodology: G.O., B.M.; Software: G.O.; Validation: G.O.; Formal analysis: G.O., B.M.; Investigation: G.O., B.M.; Resources: G.O., J.L.V., K.M.; Data curation: G.O.; Writing - original draft: G.O., B.M.; Writing - review & editing: G.O., B.M., J.L.V., K.M.; Visualization: G.O., B.M., K.M.; Supervision: G.O., K.M.; Project administration: G.O., K.M.; Funding acquisition: K.M.

### Funding

This research was funded in part by the Wellcome Trust [103740/Z/14/Z and 108905/B/15/Z], the 'Supporting Evidence Based Interventions', Bill and Melinda Gates foundation, and a Royal Society GCRF Challenge grant CH160034, each awarded to K.M.; K.M. was supported by a Wellcome Trust Investigator award grant [103740/Z/14/Z]; G.O. by a Wellcome Trust PhD studentship [108905/B/15/Z], and J.L.V. by a Royal Society GCRF Challenge grant [CH160034]. Open Access funding provided by University of Edinburgh. Deposited in PMC for immediate release.

### Data availability

*T. melophagium* DNA and RNA sequencing data, along with the draft genome assembly and its annotation, can be found under the NCBI BioProject PRJNA786535. The *T. melophagium* genome analysed in this study refers to version GCA\_022059095.1.

### References

- Akashi, H. (1994). Synonymous codon usage in drosophila-melanogaster - natural selection and translational accuracy. *Genetics* **136**, 927-935. doi:10.1093/genetics/136.3.927
- Alsford, S., Turner, D. J., Obado, S. O., Sanchez-Flores, A., Glover, L., Berriman, M., Hertz-Fowler, C. and Horn, D. (2011). High-throughput phenotyping using parallel sequencing of RNA interference targets in the African trypanosome. *Genome Res.* **21**, 915-924. doi:10.1101/gr.115089.110
- Aslett, M., Aurrecochea, C., Berriman, M., Brestelli, J., Brunk, B. P., Carrington, M., Depledge, D. P., Fischer, S., Gajria, B., Gao, X. et al. (2010). TriTrypDB: a functional genomic resource for the Trypanosomatidae. *Nucleic Acids Res.* **38**, D457-D462. doi:10.1093/nar/gkp851
- Barnett, D. W., Garrison, E. K., Quinlan, A. R., Stromberg, M. P. and Marth, G. T. (2011). BamTools: a C++ API and toolkit for analyzing and managing BAM files. *Bioinformatics* **27**, 1691-1692. doi:10.1093/bioinformatics/btr174
- Berriman, M., Ghedin, E., Hertz-Fowler, C., Blandin, G., Renaud, H., Bartholomeu, D. C., Lennard, N. J., Caler, E., Hamlin, N. E., Haas, B. et al. (2005). The genome of the African trypanosome *Trypanosoma brucei*. *Science* **309**, 416-422. doi:10.1126/science.1112642

- Bolger, A. M., Lohse, M. and Usadel, B.** (2014). Trimmomatic: a flexible trimmer for Illumina sequence data. *Bioinformatics* **30**, 2114-2120. doi:10.1093/bioinformatics/btu170
- Borst, P.** (2002). Antigenic variation and allelic exclusion. *Cell* **109**, 5-8. doi:10.1016/S0092-8674(02)00711-0
- Borst, P. and Fasel-Fowler, F.** (1979). The maxi-circle of *Trypanosoma brucei* kinetoplast DNA. *Biochim. Biophys. Acta* **565**, 1-12. doi:10.1016/0005-2787(79)90078-9
- Böse, R. and Heister, N. C.** (1993). Development of *Trypanosoma (M.) theileri* in tabanids. *J. Eukaryot. Microbiol.* **40**, 788-792. doi:10.1111/j.1550-7408.1993.tb04475.x
- Brůna, T., Hoff, K. J., Lomsadze, A., Stanke, M. and Borodovsky, M.** (2021). BRAKER2: automatic eukaryotic genome annotation with GeneMark-EP+ and AUGUSTUS supported by a protein database. *NAR Genom Bioinform* **3**, lqaa108. doi:10.1093/nargab/lqaa108
- Brůna, T., Lomsadze, A. and Borodovsky, M.** (2020). GeneMark-EP+: eukaryotic gene prediction with self-training in the space of genes and proteins. *NAR Genom Bioinform* **2**, lqaa026. doi:10.1093/nargab/lqaa026
- Buchfink, B., Xie, C. and Huson, D. H.** (2015). Fast and sensitive protein alignment using DIAMOND. *Nat. Methods* **12**, 59-60. doi:10.1038/nmeth.3176
- Burki, F.** (2014). The eukaryotic tree of life from a global phylogenomic perspective. *Cold Spring Harb. Perspect. Biol.* **6**, a016147. doi:10.1101/cshperspect.a016147
- Buscaglia, C. A., Campo, V. A., Frasc, A. C. and Di Noia, J. M.** (2006). *Trypanosoma cruzi* surface mucins: host-dependent coat diversity. *Nat. Rev. Microbiol.* **4**, 229-236. doi:10.1038/nrmicro1351
- Cabanettes, F. and Klopp, C.** (2018). D-GENIES: dot plot large genomes in an interactive, efficient and simple way. *PeerJ* **6**, e4958. doi:10.7717/peerj.4958
- Cavalier-Smith, T.** (2010). Kingdoms Protozoa and Chromista and the eozoan root of the eukaryotic tree. *Biol. Lett.* **6**, 342-345. doi:10.1098/rsbl.2009.0948
- Cayla, M., Rojas, F., Silvester, E., Venter, F. and Matthews, K. R.** (2019). African trypanosomes. *Parasit. Vectors* **12**, 190. doi:10.1186/s13071-019-3355-5
- Cayla, M., McDonald, L., MacGregor, P. and Matthews, K.** (2020). An atypical DYRK kinase connects quorum-sensing with posttranscriptional gene regulation in *Trypanosoma brucei*. *Elife* **9**, e51620. doi:10.7554/eLife.51620
- Chainey, J. E.** (1993). Horse-flies, deer-flies and clegs (Tabanidae). In *Medical Insects and Arachnids* (ed. R. P. Lane and R. W. Crosskey), pp. 310-332. Dordrecht: Springer Netherlands.
- Chan, P. P., Lin, B. Y., Mak, A. J. and Lowe, T. M.** (2021). tRNAscan-SE 2.0: improved detection and functional classification of transfer RNA genes. *Nucleic Acids Res.* **49**, 9077-9096. doi:10.1093/nar/gkab688
- Clayton, C.** (2019). Regulation of gene expression in trypanosomatids: living with polycistronic transcription. *Open Biol.* **9**, 190072. doi:10.1098/rsob.190072
- Cooper, D. and Eleftherianos, I.** (2017). Memory and specificity in the insect immune system: current perspectives and future challenges. *Front Immunol* **8**, 539. doi:10.3389/fimmu.2017.00539
- Daniels, J. P., Gull, K. and Wickstead, B.** (2010). Cell biology of the trypanosome genome. *Microbiol. Mol. Biol. Rev.* **74**, 552-569. doi:10.1128/MMBR.00024-10
- Doherty, M. L., Windle, H., Voorheis, H. P., Larkin, H., Casey, M., Clerly, D. and Murray, M.** (1993). Clinical disease associated with *Trypanosoma theileri* infection in a calf in Ireland. *Vet. Rec.* **132**, 653-656. doi:10.1136/vr.132.26.653
- Domingo-Sananes, M. R., Szöör, B., Ferguson, M. A., Urbaniak, M. D. and Matthews, K. R.** (2015). Molecular control of irreversible bistability during trypanosome developmental commitment. *J. Cell Biol.* **211**, 455-468. doi:10.1083/jcb.201506114
- Ellinghaus, D., Kurtz, S. and Willhoeft, U.** (2008). LTRharvest, an efficient and flexible software for de novo detection of LTR retrotransposons. *BMC Bioinformatics* **9**, 18. doi:10.1186/1471-2105-9-18
- Emms, D. M. and Kelly, S.** (2017). STRIDE: species tree root inference from gene duplication events. *Mol. Biol. Evol.* **34**, 3267-3278. doi:10.1093/molbev/msx259
- Emms, D. M. and Kelly, S.** (2018). STAG: Species tree inference from all genes. *BioRxiv*.
- Emms, D. M. and Kelly, S.** (2019). OrthoFinder: phylogenetic orthology inference for comparative genomics. *Genome Biol.* **20**, 238. doi:10.1186/s13059-019-1832-y
- Emms, D. M. and Kelly, S.** (2020). Benchmarking orthogroup inference accuracy: revisiting orthobench. *Genome Biol. Evol.* **12**, 2258-2266. doi:10.1093/gbe/evaa211
- Erben, E. D., Fadda, A., Lueong, S., Hoheisel, J. D. and Clayton, C.** (2014). A genome-wide tethering screen reveals novel potential post-transcriptional regulators in *Trypanosoma brucei*. *PLoS Pathog.* **10**, e1004178. doi:10.1371/journal.ppat.1004178
- Eyrewalker, A. C.** (1991). An analysis of codon usage in mammals - selection or mutation bias. *J. Mol. Evol.* **33**, 442-449. doi:10.1007/BF02103136
- Farrar, R. G. and Klei, T. R.** (1990). Prevalence of *Trypanosoma theileri* in Louisiana cattle. *J. Parasitol.* **76**, 734-736. doi:10.2307/3282992
- Flu, P. C.** (1908). Über die Flagellaten im Darm von *Melophagus ovinus*. *Arch. f. Protist.* **12**, 147-153.
- Flynn, J. M., Hubley, R., Goubert, C., Rosen, J., Clark, A. G., Feschotte, C. and Smit, A. F.** (2020). RepeatModeler2 for automated genomic discovery of transposable element families. *Proc. Natl. Acad. Sci. USA* **117**, 9451-9457. doi:10.1073/pnas.1921046117
- Funk, S., Nishiura, H., Heesterbeek, H., Edmunds, W. J. and Checchi, F.** (2013). Identifying transmission cycles at the human-animal interface: the role of animal reservoirs in maintaining gambiense human african trypanosomiasis. *PLoS Comput. Biol.* **9**, e1002855. doi:10.1371/journal.pcbi.1002855
- Gale, M., Jr, Carter, V. and Parsons, M.** (1994). Translational control mediates the developmental regulation of the *Trypanosoma brucei* Nrk protein kinase. *J. Biol. Chem.* **269**, 31659-31665. doi:10.1016/S0021-9258(18)31746-0
- Gale, M., Jr and Parsons, M.** (1993). A *Trypanosoma brucei* gene family encoding protein kinases with catalytic domains structurally related to Nek1 and NIMA. *Mol. Biochem. Parasitol.* **59**, 111-121. doi:10.1016/0166-6851(93)90012-M
- Gibson, W., Pilkington, J. G. and Pemberton, J. M.** (2010). *Trypanosoma melophagium* from the sheep ked *Melophagus ovinus* on the island of St Kilda. *Parasitology* **137**, 1799-1804. doi:10.1017/S0031182010000752
- Gotoh, O.** (2008). A space-efficient and accurate method for mapping and aligning cDNA sequences onto genomic sequence. *Nucleic Acids Res.* **36**, 2630-2638. doi:10.1093/nar/gkn105
- Hoare, C. A.** (1923). An experimental study of the sheep-trypanosome (*T. melophagium* Flu, 1908), and its transmission by the sheep-ked (*Melophagus ovinus* L.). *Parasitology* **15**, 365-424. doi:10.1017/S0031182000014888
- Hoare, C. A.** (1929). Studies on *Trypanosoma grayi*. II. Experimental transmission to the crocodile. *Trans. R. Soc. Trop. Med. Hyg.* **23**, 39-56. doi:10.1016/S0035-9203(29)90831-2
- Hoare, C. A.** (1931). Studies on *Trypanosoma grayi*. III. Life-cycle in the tsetse-fly and in the crocodile. *Parasitology* **23**, 449-484. doi:10.1017/S0031182000013858
- Hoare, C. A.** (1972). *The Trypanosomes of Mammals. A Zoological Monograph*. Oxford, England: Blackwell.
- Hoff, K. J., Lange, S., Lomsadze, A., Borodovsky, M. and Stanke, M.** (2016). BRAKER1: unsupervised RNA-Seq-based genome annotation with GeneMark-ET and AUGUSTUS. *Bioinformatics* **32**, 767-769. doi:10.1093/bioinformatics/btv661
- Hoff, K. J., Lomsadze, A., Borodovsky, M. and Stanke, M.** (2019). Whole-genome annotation with BRAKER. *Methods Mol. Biol.* **1962**, 65-95. doi:10.1007/978-1-4939-9173-0\_5
- Hu, H., Gao, J., He, J., Yu, B., Zheng, P., Huang, Z. Q., Mao, X. B., Yu, J., Han, G. Q. and Chen, D. W.** (2013). Codon optimization significantly improves the expression level of a keratinase gene in *pichia pastoris*. *PLoS One* **8**, e58393. doi:10.1371/journal.pone.0058393
- Iwata, H. and Gotoh, O.** (2012). Benchmarking spliced alignment programs including Spaln2, an extended version of Spaln that incorporates additional species-specific features. *Nucleic Acids Res.* **40**, e161. doi:10.1093/nar/gks708
- Jaskowska, E., Butler, C., Preston, G. and Kelly, S.** (2015). Phytomonas: trypanosomatids adapted to plant environments. *PLoS Pathog.* **11**, e1004484. doi:10.1371/journal.ppat.1004484
- Jones, N. G., Thomas, E. B., Brown, E., Dickens, N. J., Hammarton, T. C. and Mottram, J. C.** (2014a). Regulators of *Trypanosoma brucei* cell cycle progression and differentiation identified using a kinome-wide RNAi screen. *PLoS Pathog.* **10**, e1003886. doi:10.1371/journal.ppat.1003886
- Jones, P., Binns, D., Chang, H. Y., Fraser, M., Li, W., McAnulla, C., McWilliam, H., Maslen, J., Mitchell, A., Nuka, G. et al.** (2014b). InterProScan 5: genome-scale protein function classification. *Bioinformatics* **30**, 1236-1240. doi:10.1093/bioinformatics/btu031
- Kaufer, A., Ellis, J., Stark, D. and Barratt, J.** (2017). The evolution of trypanosomatid taxonomy. *Parasit. Vectors* **10**, 287. doi:10.1186/s13071-017-2204-7
- Kelly, S., Ivens, A., Manna, P. T., Gibson, W. and Field, M. C.** (2014). A draft genome for the African crocodylian trypanosome *Trypanosoma grayi*. *Sci. Data* **1**, 140024. doi:10.1038/sdata.2014.24
- Kelly, S., Ivens, A., Mott, G. A., O'Neill, E., Emms, D., Macleod, O., Voorheis, P., Tyler, K., Clark, M., Matthews, J. et al.** (2017). An alternative strategy for trypanosome survival in the mammalian bloodstream revealed through genome and transcriptome analysis of the ubiquitous bovine parasite trypanosoma (*Megatrypanum*) *theileri*. *Genome Biol. Evol.* **9**, 2093-2109. doi:10.1093/gbe/evx152
- Kleisen, C. M. and Borst, P.** (1975). Sequence heterogeneity of the mini-circles of kinetoplast DNA of *Crithidia luciliae* and evidence for the presence of a component more complex than mini-circle DNA in the kinetoplast network. *Biochim. Biophys. Acta* **407**, 473-478. doi:10.1016/0005-2787(75)90301-9
- Kniepert, F. W.** (1980). Blood-feeding and nectar-feeding in adult tabanidae (Diptera). *Oecologia* **46**, 125-129. doi:10.1007/BF00346976
- Kriventseva, E. V., Kuznetsov, D., Teigenfeldt, F., Manni, M., Dias, R., Simão, F. A. and Zdobnov, E. M.** (2019). OrthoDB v10: sampling the diversity of animal, plant, fungal, protist, bacterial and viral genomes for evolutionary and functional annotations of orthologs. *Nucleic Acids Res.* **47**, D807-D811. doi:10.1093/nar/gky1053
- Laetsch, D. R. and Blaxter, M. L.** (2017a). KinFin: software for taxon-aware analysis of clustered protein sequences. *G3 (Bethesda)* **7**, 3349-3357. doi:10.1534/g3.117.300233

- Laetsch, D. R. and Blaxter, M. L.** (2017b). BlobTools: interrogation of genome assemblies. *F1000Research* **6**, 1287. doi:10.12688/f1000research.12232.1
- Lao, P. J. and Forsdyke, D. R.** (2000). Thermophilic bacteria strictly obey Szybalski's transcription direction rule and politely purine-load RNAs with both adenine and guanine. *Genome Res.* **10**, 228-236. doi:10.1101/gr.10.2.228
- Leger, A. and Leonardi, T.** (2019). pycQC, interactive quality control for Oxford Nanopore Sequencing. *J. Open Source Softw.* **4**, 1236. doi:10.21105/joss.01236
- Leinonen, R., Sugawara, H. and Shumway, M. and International Nucleotide Sequence Database Collaboration** (2011). The sequence read archive. *Nucleic Acids Res.* **39**, D19-D21. doi:10.1093/nar/gkq1019
- Letunic, I. and Bork, P.** (2007). Interactive Tree Of Life (iTOL): an online tool for phylogenetic tree display and annotation. *Bioinformatics* **23**, 127-128. doi:10.1093/bioinformatics/btl529
- Li, H.** (2013). Aligning sequence reads, clone sequences and assembly contigs with BWA - MEM. *arXiv:1303.3997*.
- Li, H.** (2018). Minimap2: pairwise alignment for nucleotide sequences. *Bioinformatics* **34**, 3094-3100. doi:10.1093/bioinformatics/bty191
- Li, H., Handsaker, B., Wysoker, A., Fennell, T., Ruan, J., Homer, N., Marth, G., Abecasis, G. and Durbin, R. and Genome Project Data Processing Subgroup** (2009). The sequence alignment/map format and SAMtools. *Bioinformatics* **25**, 2078-2079. doi:10.1093/bioinformatics/btp352
- Ling, A. S., Trotter, J. R. and Hendriks, E. F.** (2011). A zinc finger protein, TbZC3H20, stabilizes two developmentally regulated mRNAs in trypanosomes. *J. Biol. Chem.* **286**, 20152-20162. doi:10.1074/jbc.M110.139261
- Liu, B., Kamanyi Marucha, K. and Clayton, C.** (2020). The zinc finger proteins ZC3H20 and ZC3H21 stabilise mRNAs encoding membrane proteins and mitochondrial proteins in insect-form *Trypanosoma brucei*. *Mol. Microbiol.* **113**, 430-451. doi:10.1111/mmi.14429
- Lomsadze, A., Burns, P. D. and Borodovsky, M.** (2014). Integration of mapped RNA-Seq reads into automatic training of eukaryotic gene finding algorithm. *Nucleic Acids Res.* **42**, e119. doi:10.1093/nar/gku557
- Lueong, S., Merce, C., Fischer, B., Hoheisel, J. D. and Erben, E. D.** (2016). Gene expression regulatory networks in *Trypanosoma brucei*: insights into the role of the mRNA-binding proteome. *Mol. Microbiol.* **100**, 457-471. doi:10.1111/mmi.13328
- Marçais, G. and Kingsford, C.** (2011). A fast, lock-free approach for efficient parallel counting of occurrences of k-mers. *Bioinformatics* **27**, 764-770. doi:10.1093/bioinformatics/btr011
- Martinković, F., Matanović, K., Rodrigues, A. C., Garcia, H. A. and Teixeira, M. M.** (2012). *Trypanosoma* (Megatrypanum) melophagium in the sheep ked *Melophagus ovinus* from organic farms in Croatia: phylogenetic inferences support restriction to sheep and sheep keds and close relationship with trypanosomes from other ruminant species. *J. Eukaryot. Microbiol.* **59**, 134-144. doi:10.1111/j.1550-7408.2011.00599.x
- Maslov, D. A., Opperdoes, F. R., Kostygov, A. Y., Hashimi, H., Lukeš, J. and Yurchenko, V.** (2019). Recent advances in trypanosomatid research: genome organization, expression, metabolism, taxonomy and evolution. *Parasitology* **146**, 1-27. doi:10.1017/S0031182018000951
- Matthews, D. M., Kingston, N., Maki, L. and Nelms, G.** (1979). *Trypanosoma theileri* Laveran, 1902, in Wyoming cattle. *Am. J. Vet. Res.* **40**, 623-629.
- Mehlitz, D. and Molyneux, D. H.** (2019). The elimination of *Trypanosoma brucei* gambiense? Challenges of reservoir hosts and transmission cycles: expect the unexpected. *Parasite Epidemiol Control* **6**, e00113. doi:10.1016/j.parepi.2019.e00113
- Melville, S. E., Leech, V., Gerrard, C. S., Tait, A. and Blackwell, J. M.** (1998). The molecular karyotype of the megabase chromosomes of *Trypanosoma brucei* and the assignment of chromosome markers. *Mol. Biochem. Parasitol.* **94**, 155-173. doi:10.1016/S0166-6851(98)00054-1
- Mistry, J., Chuguransky, S., Williams, L., Qureshi, M., Salazar, G. A., Sonnhammer, E. L. L., Tosatto, S. C. E., Paladin, L., Raj, S., Richardson, L. J. et al.** (2021). Pfam: The protein families database in 2021. *Nucleic Acids Res.* **49**, D412-D419. doi:10.1093/nar/gkaa913
- Mony, B. M. and Matthews, K. R.** (2015). Assembling the components of the quorum sensing pathway in African trypanosomes. *Mol. Microbiol.* **96**, 220-232. doi:10.1111/mmi.12949
- Mony, B. M., MacGregor, P., Ivens, A., Rojas, F., Cowton, A., Young, J., Horn, D. and Matthews, K.** (2014). Genome-wide dissection of the quorum sensing signalling pathway in *Trypanosoma brucei*. *Nature* **505**, 681-685. doi:10.1038/nature12864
- Mott, G. A., Wilson, R., Fernando, A., Robinson, A., MacGregor, P., Kennedy, D., Schaap, D., Matthews, J. B. and Matthews, K. R.** (2011). Targeting cattle-borne zoonoses and cattle pathogens using a novel trypanosomatid-based delivery system. *PLoS Pathog.* **7**, e1002340. doi:10.1371/journal.ppat.1002340
- Müller, I. B., Domenicali-Pfister, D., Roditi, I. and Vassella, E.** (2002). Stage-specific requirement of a mitogen-activated protein kinase by *Trypanosoma brucei*. *Mol. Biol. Cell* **13**, 3787-3799. doi:10.1091/mbc.e02-02-0093
- Nardy, A. F., Freire-de-Lima, C. G., Pérez, A. R. and Morrot, A.** (2016). Role of *trypanosoma cruzi* trans-sialidase on the escape from host immune surveillance. *Front. Microbiol.* **7**, 348. doi:10.3389/fmicb.2016.00348
- Nielsen, H.** (2017). Predicting secretory proteins with SignalP. *Methods Mol. Biol.* **1611**, 59-73. doi:10.1007/978-1-4939-7015-5\_6
- Novoa, E. M. and de Poupiana, L. R.** (2012). Speeding with control: codon usage, tRNAs, and ribosomes. *Trends Genet.* **28**, 574-581. doi:10.1016/j.tig.2012.07.006
- Oldrieve, G., Verney, M., Jaron, K. S., Hebert, L. and Matthews, K. R.** (2021). Monomorphic *Trypanosoma*: towards reconciling phylogeny and pathologies. *Microb. Genom.* **7**, 000632. doi:10.1099/mgen.0.000632
- Parsons, M., Nelson, R. G., Watkins, K. P. and Agabian, N.** (1984). Trypanosome mRNAs share a common 5' spliced leader sequence. *Cell* **38**, 309-316. doi:10.1016/0092-8674(84)90552-X
- Pays, E., Vanhamme, L. and Pérez-Morga, D.** (2004). Antigenic variation in *Trypanosoma brucei*: facts, challenges and mysteries. *Curr. Opin. Microbiol.* **7**, 369-374. doi:10.1016/j.mib.2004.05.001
- Paz, A., Mester, D., Baca, I., Nevo, E. and Korol, A.** (2004). Adaptive role of increased frequency of polypurine tracts in mRNA sequences of thermophilic prokaryotes. *Proc. Natl. Acad. Sci. U.S.A.* **101**, 2951-2956. doi:10.1073/pnas.0308594100
- Peacock, L., Kay, C., Farren, C., Bailey, M., Carrington, M. and Gibson, W.** (2021). Sequential production of gametes during meiosis in trypanosomes. *Commun. Biol.* **4**, 555. doi:10.1038/s42003-021-02058-5
- Plotkin, J. B., Robins, H. and Levine, A. J.** (2004). Tissue-specific codon usage and the expression of human genes. *Proc. Natl. Acad. Sci. U.S.A.* **101**, 12588-12591. doi:10.1073/pnas.0404957101
- Podlipaev, S.** (2001). The more insect trypanosomatids under study-the more diverse *Trypanosomatidae* appears. *Int. J. Parasitol.* **31**, 648-652. doi:10.1016/S0020-7519(01)00139-4
- Pool, J. E. and Nielsen, R.** (2007). Population size changes reshape genomic patterns of diversity. *Evolution* **61**, 3001-3006. doi:10.1111/j.1558-5646.2007.00238.x
- Porter, A.** (1910). The Structure and Life-History of *Crithidia Melophagia* (Flu), an Endo-parasite of the Sheep-Ked, *Melophagus Ovinus*. *J. Cell Sci.* **218**, 189-224. doi:10.1242/jcs.s2-55.218.189
- Rao, Y. S., Wu, G. Z., Wang, Z. F., Chai, X. W., Nie, Q. H. and Zhang, X. Q.** (2011). Mutation bias is the driving force of codon usage in the *Gallus gallus* genome. *DNA Res.* **18**, 499-512. doi:10.1093/dnares/dsr035
- Ruan, J. and Li, H.** (2020). Fast and accurate long-read assembly with wtdbg2. *Nat. Methods* **17**, 155-158. doi:10.1038/s41592-019-0669-3
- Sanchez-Moreno, M., Laszity, D., Coppens, I. and Opperdoes, F. R.** (1992). Characterization of carbohydrate metabolism and demonstration of glycosomes in a *Phytomonas* sp. isolated from *Euphorbia characias*. *Mol. Biochem. Parasitol.* **54**, 185-199. doi:10.1016/0166-6851(92)90111-V
- Schlafer, D. H.** (1979). *Trypanosoma theileri*: a literature review and report of incidence in New York cattle. *Cornell Vet* **69**, 411-425.
- Schnauffer, A., Domingo, G. J. and Stuart, K.** (2002). Natural and induced dyskinetoplastic trypanosomatids: how to live without mitochondrial DNA. *Int. J. Parasitol.* **32**, 1071-1084. doi:10.1016/S0020-7519(02)00020-6
- Seiff, H. A.** (1995). Clinical trypanosomiasis due to *trypanosoma-theileri* in a cow in iran. *Trop. Anim. Health Prod.* **27**, 93-94. doi:10.1007/BF02236319
- Seppie, M., Manni, M. and Zdobnov, E. M.** (2019). BUSCO: assessing genome assembly and annotation completeness. *Methods Mol. Biol.* **1962**, 227-245. doi:10.1007/978-1-4939-9173-0\_14
- Serpil, N. and Zafer, K.** (2008). *Trypanosoma melophagium* in blood cell culture. *Ank. Üniv. Vet. Fak. Derg.* **50**, 1-1. doi:10.1501/Vetfak\_0000000325
- Seward, E. A. and Kelly, S.** (2016). Dietary nitrogen alters codon bias and genome composition in parasitic microorganisms. *Genome Biol.* **17**, 226. doi:10.1186/s13059-016-1087-9
- Seward, E. A. and Kelly, S.** (2018). Selection-driven cost-efficiency optimization of transcripts modulates gene evolutionary rate in bacteria. *Genome Biol.* **19**, 102. doi:10.1186/s13059-018-1480-7
- Shah, P. and Gilchrist, M. A.** (2011). Explaining complex codon usage patterns with selection for translational efficiency, mutation bias, and genetic drift. *Proc. Natl. Acad. Sci. U.S.A.* **108**, 10231-10236. doi:10.1073/pnas.1016719108
- Simpson, L.** (1979). Isolation of maxicircle component of kinetoplast DNA from hemoflagellate protozoa. *Proc. Natl. Acad. Sci. USA* **76**, 1585-1588. doi:10.1073/pnas.76.4.1585
- Sorensen, M. A., Kurland, C. G. and Pedersen, S.** (1989). Codon usage determines translation rate in *Escherichia coli*. *J. Mol. Biol.* **207**, 365-377. doi:10.1016/0022-2836(89)90260-X
- Stanke, M., Schöffmann, O., Morgenstern, B. and Waack, S.** (2006). Gene prediction in eukaryotes with a generalized hidden Markov model that uses hints from external sources. *BMC Bioinformatics* **7**, 62. doi:10.1186/1471-2105-7-62
- Stanke, M., Diekhans, M., Baertsch, R. and Haussler, D.** (2008). Using native and synthetically mapped cDNA alignments to improve de novo gene finding. *Bioinformatics* **24**, 637-644. doi:10.1093/bioinformatics/btn013
- Steinert, M.** (1960). Mitochondria associated with the kinetoplast of *trypanosoma mega*. *J. Biophys. Biochem. Cytol.* **8**, 542-546. doi:10.1083/jcb.8.2.542

- Swingle, L. D.** (1911). The relation of crithidia melophagia to the sheep's blood, with remarks upon the controversy between Dr. Porter and Dr. Woodcock. *Trans. Am. Microsc. Soc.* **30**, 275. doi:10.2307/3221144
- Szöőr, B., Wilson, J., McElhinney, H., Taberner, L. and Matthews, K. R.** (2006). Protein tyrosine phosphatase TbPTP1: A molecular switch controlling life cycle differentiation in trypanosomes. *J. Cell Biol.* **175**, 293-303. doi:10.1083/jcb.200605090
- Szöőr, B., Ruberto, I., Burchmore, R. and Matthews, K. R.** (2010). A novel phosphatase cascade regulates differentiation in *Trypanosoma brucei* via a glycosomal signaling pathway. *Genes Dev.* **24**, 1306-1316. doi:10.1101/gad.570310
- Team, R. C.** (2019). R: a language and environment for statistical computing. R Foundation for Statistical Computing.
- Toft, C. and Andersson, S. G. E.** (2010). Evolutionary microbial genomics: insights into bacterial host adaptation. *Nat. Rev. Genet.* **11**, 465-475. doi:10.1038/nrg2798
- Toh, J. Y., Nkouawa, A., Sánchez, S. R., Shi, H., Kolev, N. G. and Tschudi, C.** (2021). Identification of positive and negative regulators in the stepwise developmental progression towards infectivity in *Trypanosoma brucei*. *Sci. Rep.* **11**, 5755. doi:10.1038/s41598-021-85225-2
- Trindade, S., Rijo-Ferreira, F., Carvalho, T., Pinto-Neves, D., Guegan, F., Aresta-Branco, F., Bento, F., Young, S. A., Pinto, A., Van den Abbeele, J. et al.** (2016). *Trypanosoma brucei* parasites occupy and functionally adapt to the adipose tissue in mice. *Cell Host Microbe* **19**, 837-848. doi:10.1016/j.chom.2016.05.002
- Ullu, E., Tschudi, C. and Chakraborty, T.** (2004). RNA interference in protozoan parasites. *Cell. Microbiol.* **6**, 509-519. doi:10.1111/j.1462-5822.2004.00399.x
- Underwood, W. J., Blauwiel, R., Delano, M. L., Gillesby, R., Mischler, S. A. and Schoell, A.** (2015). Biology and diseases of ruminants (sheep, goats, and cattle). In *Laboratory Animal Medicine*, pp. 623-694: Elsevier.
- Vaser, R., Sović, I., Nagarajan, N. and Sikic, M.** (2017). Fast and accurate de novo genome assembly from long uncorrected reads. *Genome Res.* **27**, 737-746. doi:10.1101/gr.214270.116
- Vurture, G. W., Sedlazeck, F. J., Nattestad, M., Underwood, C. J., Fang, H., Gurtowski, J. and Schatz, M. C.** (2017). GenomeScope: fast reference-free genome profiling from short reads. *Bioinformatics* **33**, 2202-2204. doi:10.1093/bioinformatics/btx153
- Walker, B. J., Abeel, T., Shea, T., Priest, M., Abouelliel, A., Sakthikumar, S., Cuomo, C. A., Zeng, Q., Wortman, J., Young, S. K. et al.** (2014). Pilon: an integrated tool for comprehensive microbial variant detection and genome assembly improvement. *PLoS One* **9**, e112963. doi:10.1371/journal.pone.0112963
- Walrad, P., Paterou, A., Acosta-Serrano, A. and Matthews, K. R.** (2009). Differential trypanosome surface coat regulation by a CCCH protein that co-associates with procyclin mRNA cis-elements. *PLoS Pathog.* **5**, e1000317. doi:10.1371/journal.ppat.1000317
- Wang, F., Ekiert, D. C., Ahmad, I., Yu, W., Zhang, Y., Bazirgan, O., Torkamani, A., Raudsepp, T., Mwangi, W., Criscitiello, M. F. et al.** (2013). Reshaping antibody diversity. *Cell* **153**, 1379-1393. doi:10.1016/j.cell.2013.04.049
- Wickstead, B., Ersfeld, K. and Gull, K.** (2004). The small chromosomes of *Trypanosoma brucei* involved in antigenic variation are constructed around repetitive palindromes. *Genome Res.* **14**, 1014-1024. doi:10.1101/gr.2227704
- Yao, C. Q.** (2010). Major surface protease of trypanosomatids: one size fits all? *Infect. Immun.* **78**, 22-31. doi:10.1128/IAI.00776-09

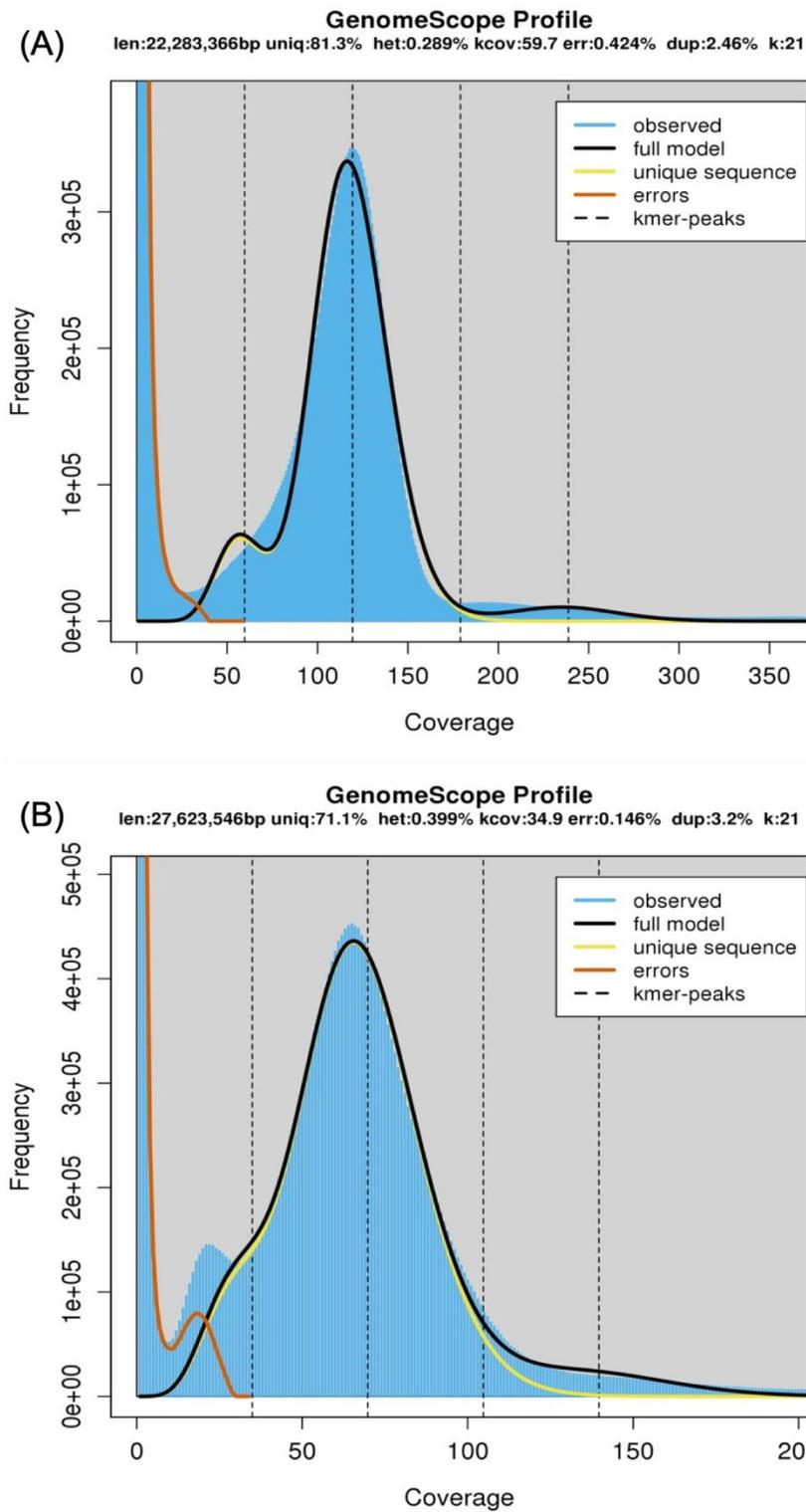


**Fig. S1.** k-mer spectra of (A) *T. melophagium* and (B) *T. theileri* using a k-mer size of 21. The statistics presented in these images represent the lowest estimate size, the highest estimate was used in Table 1 as these had a greater model fit.

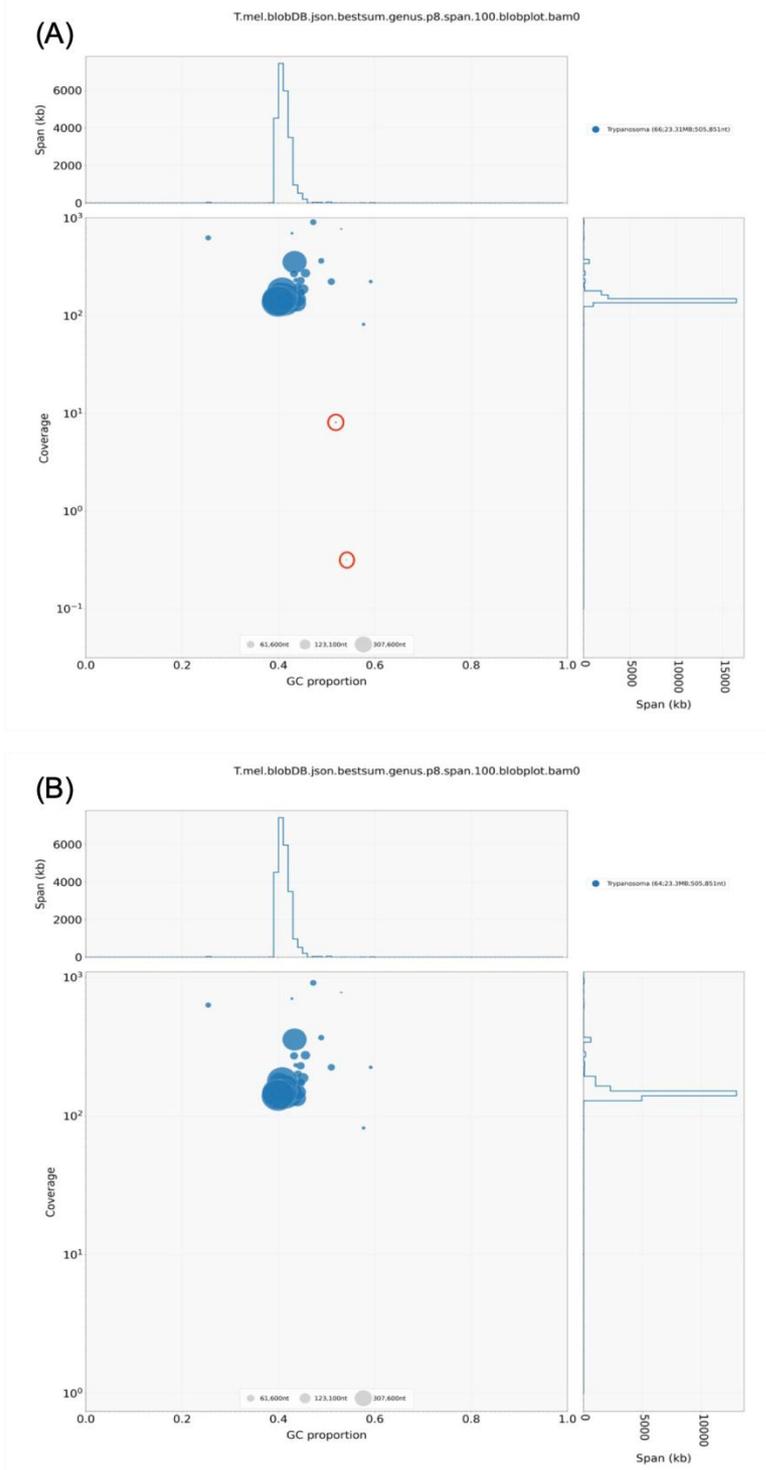


**Fig. S2.** Coverage and blast annotation for (A) the polished assembly and (B) the manually trimmed assembly.

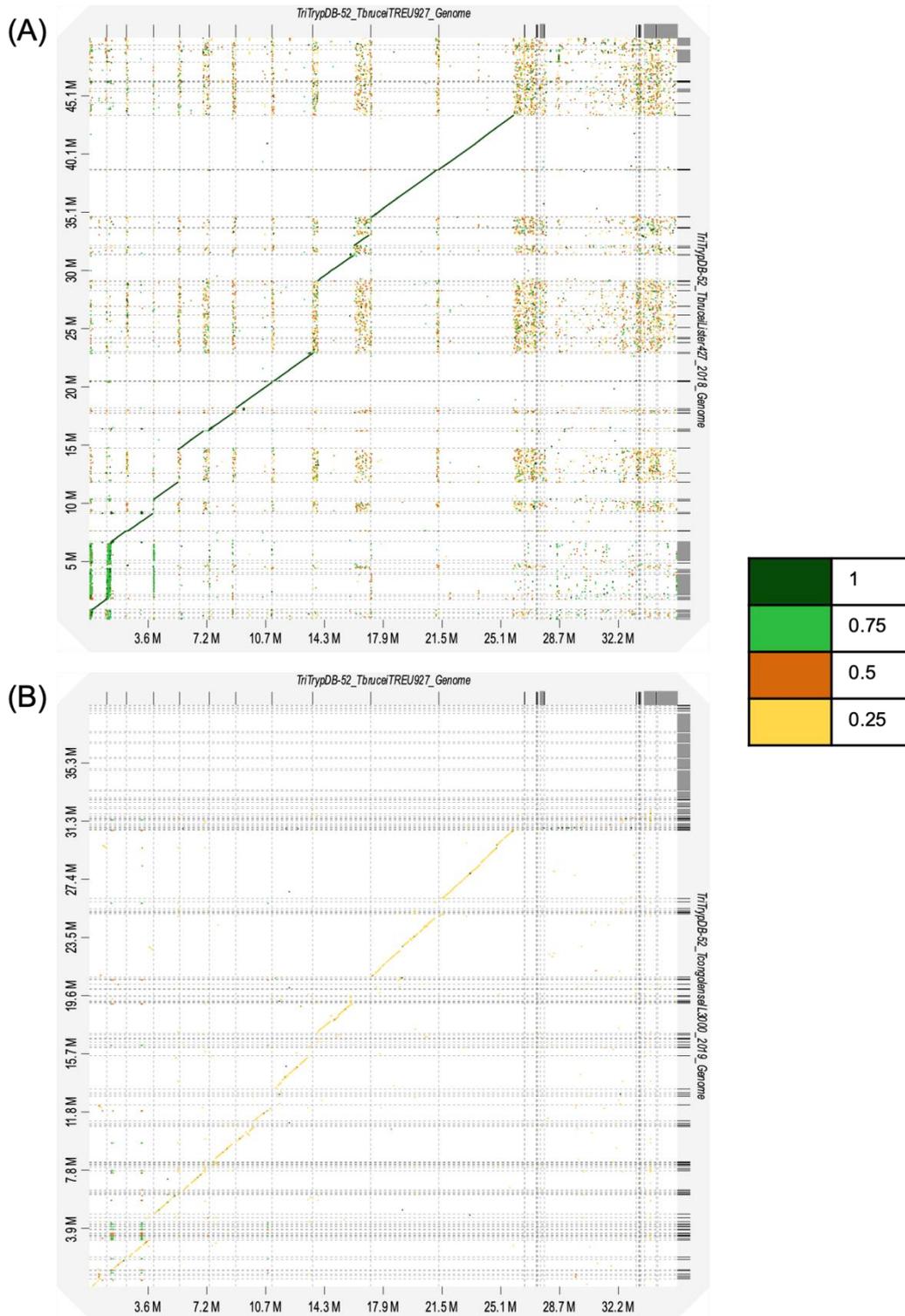


**Fig. S3.** Synteny plot of (A) *T. brucei* TREU927/4 and *T. brucei* Lister 427 (2018) and (B) *T. brucei* TREU927/4 and *T. congolense* IL3000 2019 genome sequences. The legend refers to the identity between the sequences.

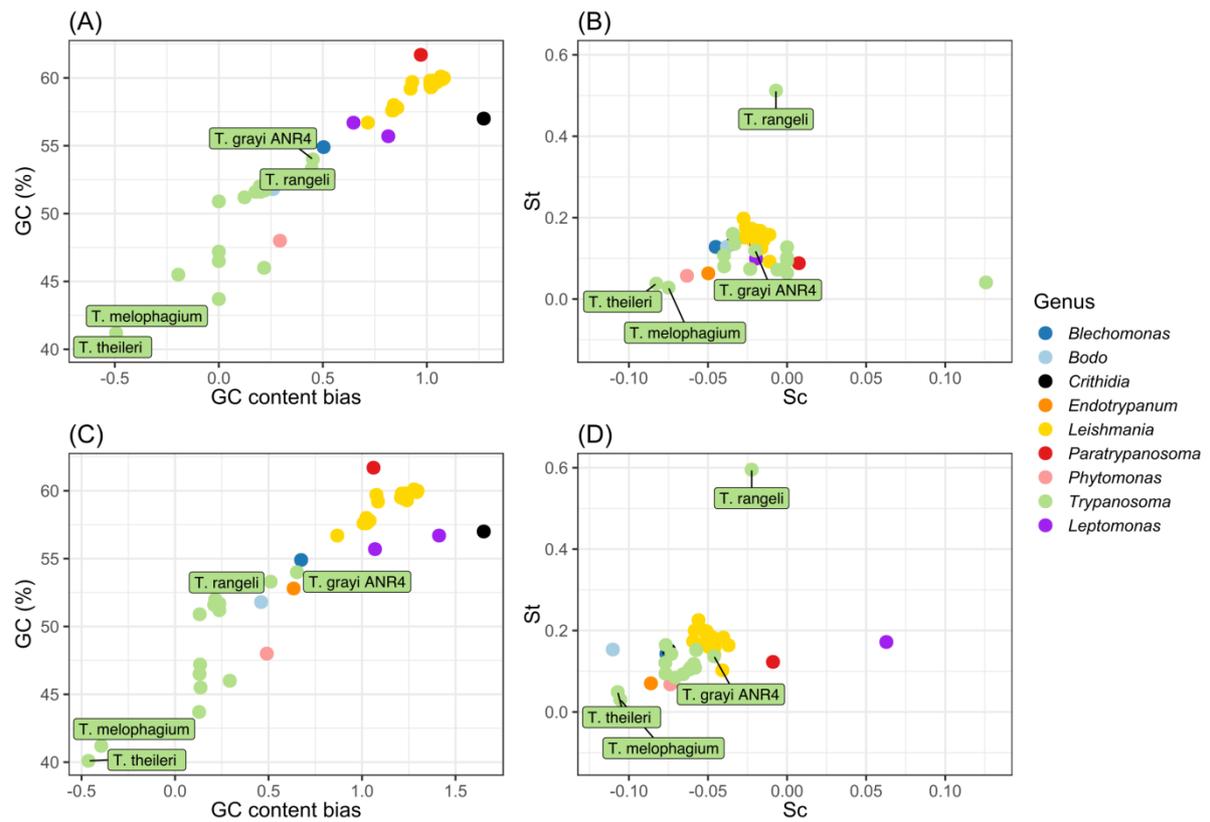


**Fig. S4.** (A) GC content across the whole genome and GC content bias in a every CDS. (B) Selection acting on translational efficiency (St) and selection acting on nucleotide cost (Sc). (C) GC content across the whole genome and GC content bias in CDS of a trypanosomatid universal single copy orthologue which is essential in every life cycle stage in *T. brucei* (n=158). (D) Selection acting on translational efficiency (St) and selection acting on nucleotide cost (Sc) in trypanosomatid universal single copy orthologues which is essential in every life cycle stage in *T. brucei* (n=158).

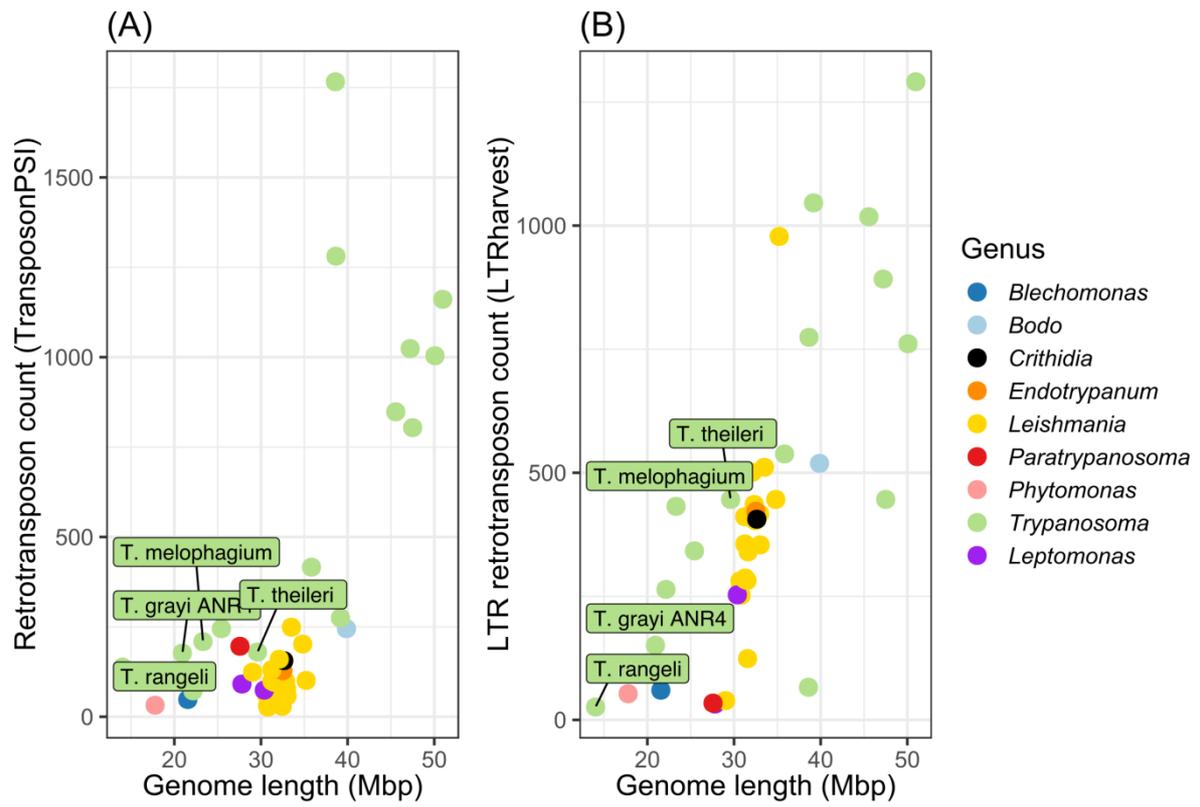


**Fig. S5.** (A) Retrotransposon (B) long terminal repeat (LTR) retrotransposon counts compared to genome length.

**Table S1.** Software and any options used.

<b>Tool</b>	<b>Version</b>	<b>Flag</b>	<b>Available at</b>
<b>Guppy</b>	4.0.15	--flowcell FLO-MIN106 --kit SQK-RAD004	<a href="https://community.nanoporetech.com/">https://community.nanoporetech.com/</a>
<b>PycoQC</b>	2.5.0.3		<a href="https://github.com/arslanslide/pycoQC">https://github.com/arslanslide/pycoQC</a>
<b>Trimmomatic</b>	0.39	-SLIDINGWINDOW 4:20 -MINLEN 50	<a href="https://github.com/timflutre/trimmomatic">https://github.com/timflutre/trimmomatic</a>
<b>GenomeScope</b>	1	-Kmer 21 -Max kmer cov. 1000	<a href="http://qb.cshl.edu/genomescope/">http://qb.cshl.edu/genomescope/</a>
<b>Jellyfish</b>	2.2.10	-C -m 21 -s 1000000000	<a href="https://github.com/gmarcais/Jellyfish">https://github.com/gmarcais/Jellyfish</a>
<b>Wtdbg2</b>	3	-x ont -g 30m -A -t 10	<a href="https://github.com/ruanjue/wtdbg2">https://github.com/ruanjue/wtdbg2</a>
<b>Minimap2</b>	2.17-r941	-ax map-ont	<a href="https://github.com/lh3/minimap2">https://github.com/lh3/minimap2</a>
<b>Racon</b>	v1.4.13	-m 8 -x -6 -g -8 -w 500	<a href="https://github.com/isovic/racon">https://github.com/isovic/racon</a>
<b>Medaka</b>	V5	-m r941_min_high_g360	<a href="https://github.com/nanoporetech/medaka">https://github.com/nanoporetech/medaka</a>
<b>BWA-MEM</b>	0.7.17-r1188		<a href="https://github.com/lh3/bwa">https://github.com/lh3/bwa</a>
<b>Pilon</b>	1.24	--genome --diploid -bam --bam	<a href="https://github.com/broadinstitute/pilon">https://github.com/broadinstitute/pilon</a>
<b>Blast</b>	2.6.0+	blastn -task megablast -outfmt '6 qseqid	<a href="ftp://ftp.ncbi.nlm.nih.gov/blast/executables/blast+/LATEST/">ftp://ftp.ncbi.nlm.nih.gov/blast/executables/blast+/LATEST/</a>

		staxids bitscore std' -max_target_seqs 1 -max_hsps 1 -evaluate 1e-25 or 1e-5	
<b>DIAMOND</b>	2.0.5.14 3	Blastx --sensitive --max-target-seqs 1 --evaluate 1e-25	<a href="http://www.diamondsearch.org">http://www.diamondsearch.org</a>
<b>BlobTools</b>	1.1.1	-r genus	<a href="https://github.com/DRL/blobtools">https://github.com/DRL/blobtools</a>
<b>Scaffold_stats.pl</b>	N/A		<a href="https://github.com/sujaikumar/semblage">https://github.com/sujaikumar/semblage</a>
<b>BUSCO</b>	V5	-l euglenozoa_odb10	<a href="https://busco.ezlab.org/">https://busco.ezlab.org/</a>
<b>RepeatModeler</b>	N/A	-database - LTRStruct -pa 8	<a href="http://www.repeatmasker.org/RepeatModeler/">http://www.repeatmasker.org/RepeatModeler/</a>
<b>RepeatMasker</b>	N/A	-lib consensi.fa.classified -pa 8 -xsmall -nolow -gff	<a href="http://www.repeatmasker.org/RMDownload.html">http://www.repeatmasker.org/RMDownload.html</a>
<b>BRAKER2</b>	2.1.6	--prot_seq --bam --softmasking --etpmode --gff3	<a href="https://github.com/Gaius-Augustus/BRAKER">https://github.com/Gaius-Augustus/BRAKER</a>
<b>D-Genies</b>	1.2.0	-Minimap2	<a href="http://dgenies.toulouse.inra.fr/run">http://dgenies.toulouse.inra.fr/run</a>
<b>tRNAscan-SE</b>	2.0.9	-E	<a href="http://lowelab.ucsc.edu/tRNAscan-SE/">http://lowelab.ucsc.edu/tRNAscan-SE/</a>
<b>CodonMuse</b>	0.1.0	-f -tscan	<a href="https://github.com/easeward/CodonMuSe">https://github.com/easeward/CodonMuSe</a>

<b>TransposonPSI</b>	1.0.0	-nuc	<a href="http://transposonpsi.sourceforge.net">http://transposonpsi.sourceforge.net</a>
<b>gt suffixerator</b>	1.6.2	-tis -suf -lcp -des -ssp -sds -dna	<a href="http://genometools.org/tools/gt_ltrharvest.html">http://genometools.org/tools/gt_ltrharvest.html</a>
<b>gt LTRharvest</b>	1.6.2		<a href="http://genometools.org/tools/gt_ltrharvest.html">http://genometools.org/tools/gt_ltrharvest.html</a>
<b>OrthoFinder</b>	2.5.2	-S diamond_ultra_sens	<a href="https://github.com/davidemms/OrthoFinder">https://github.com/davidemms/OrthoFinder</a>
<b>InterProScan</b>	5.52-86.0	--dp --goterms -appl SignalP-EUK-4.1, Pfam -f TSV	<a href="https://www.ebi.ac.uk/interpro/">https://www.ebi.ac.uk/interpro/</a>
<b>KinFin</b>	1.0.3		<a href="https://github.com/DRL/kinfin">https://github.com/DRL/kinfin</a>
<b>iTOL</b>	6		<a href="https://itol.embl.de">https://itol.embl.de</a>
<b>R</b>	3.6.1		<a href="https://www.r-project.org/">https://www.r-project.org/</a>
<b>ggplot2</b>	3.3.3		<a href="https://cran.r-project.org/web/packages/ggplot2/index.html">https://cran.r-project.org/web/packages/ggplot2/index.html</a>
<b>ggrepel</b>	0.9.1		<a href="https://cran.r-project.org/web/packages/ggrepel/index.html">https://cran.r-project.org/web/packages/ggrepel/index.html</a>

**Table S2.**

[Click here to download Table S2](#)

**Table S3.**

[Click here to download Table S3](#)

**Table S4.**

[Click here to download Table S4](#)

**Table S5.**

[Click here to download Table S5](#)